SEA-LEVEL CHANGE DURING THE LAST 2500 YEARS IN NEW JERSEY, USA

Andrew C. Kemp[1*], Benjamin P. Horton[2], Christopher H. Vane[3], Christopher E. Bernhardt[4], D. Reide Corbett[5], Simon E. Engelhart[6], Shimon C. Anisfeld[7], Andrew C. Parnell[8], and Niamh Cahill[8]

1. Department of Earth and Ocean Sciences, Tufts University, Medford, MA 02155, USA

2. Institute of Marine and Coastal Sciences, Rutgers University, New Brunswick, NJ 08901, USA

3. British Geological Survey, Keyworth, Nottingham NG12 5GG, UK

4. United States Geological Survey, National Center, Reston, VA 20192, USA

5. Department of Geological Science, East Carolina University, Greenville, NC 27858, USA

6. Department of Geosciences, University of Rhode Island, Kingston, RI 02881, USA

7. School of Forestry and Environmental Studies, Yale University, New Haven, CT 06511, USA

8. School of Mathematical Sciences (Statistics), Complex Adaptive Systems Laboratory, University College Dublin, Belfield, Dublin 4, Ireland

* *Corresponding author:* andrew.kemp@tufts.edu; 617 627 0869

Abstract

Relative sea-level changes during the last ~2500 years in New Jersey, USA were reconstructed to test if late Holocene sea level was stable or included persistent and distinctive phases of variability. Foraminifera and bulk-sediment $\delta^{13}C$ values were combined to reconstruct paleomarsh elevation with decimeter precision from sequences of salt-marsh sediment at two sites using a multi-proxy approach. The history of sediment deposition was constrained by a composite chronology. An age-depth model developed for each core enabled reconstruction of sea level with multi-decadal resolution. Following correction for land-level change (1.4mm/yr), four successive and sustained (multi-centennial) sea-level trends were objectively identified and quantified using error-in-variables change point analysis to account for age and sea-level uncertainties. From at least 500BC to 250AD sea-level fell at 0.11mm/yr. The second period saw sea-level rise at 0.62mm/yr from 250AD to 733AD. Between 733AD and 1850AD sea level fell at 0.12mm/yr. The reconstructed rate of sea-level rise since ~1850AD was 3.1mm/yr and represents the most rapid period of change for at least 2500 years. This trend began between 1830AD and 1873AD and its onset is synchronous with other locations on the U.S. Atlantic coast. Since this change point, reconstructed sea-level rise is in agreement with regional tide-gauge records and exceeds the global average estimate for the 20th century. These positive and negative departures from background rates demonstrate that the late Holocene sea level was not stable in New Jersey.

Key words: Foraminifera, salt-marsh, transfer function, Medieval Climate Anomaly, Little Ice Age, 20th century

1. Introduction

Late Holocene (last ~2000 years) sea-level reconstructions with decimeter vertical and multi-decadal temporal resolution provide important information for investigating the relationships between sea-level change and temperature. Such data calibrate and test the validity of models that predict sea-level changes under scenarios of global climate evolution (e.g. Bittermann et al., 2013; Rahmstorf, 2007). Instrumental measurements of sea level (tide gauges and satellites) are too short to capture pre-anthropogenic trends and the long-term (100s to 1000s of years) response of sea level to temperature variations. This time-series limitation hinders the development of predictive models and is a motivation for reconstructing late Holocene sea-level changes. Proxy-temperature data show distinct climate phases during the last 2000 years such as the Medieval Climate Anomaly, Little Ice Age and 20th century warming (e.g. Ahmed et al., 2013; Mann et al., 2008; Moberg et al., 2005; Thompson et al., 2013). In contrast, relatively little is known about sea level during this period, although there is some evidence that persistent positive and negative departures from regional, linear background rates (driven primarily by glacio-isostatic adjustment; GIA) occurred prior to the onset of modern sea-level rise in the late 19th or early 20th centuries (e.g. Gehrels, 2000; González and Törnqvist, 2009; Kemp et al., 2011; Sivan et al., 2004; van de Plassche, 2000).

Salt-marsh sediment is one of the most important archives for reconstructing relative sea level (RSL) during the late Holocene. Under regimes of RSL rise salt marshes accumulate sediment to maintain their elevation in the tidal frame (Morris et al., 2002). The resulting sequences of salt-marsh sediment accurately preserve the elevation of past RSL, which is the net result of all driving mechanisms. The vertical precision of RSL reconstructions is maximized by employing sea-level indicators that differentiate among salt-marsh sub-environments to estimate the tidal elevation where the sediment was originally deposited (paleomarsh elevation; PME). Salt-marsh foraminifera are sea-level indicators because their distribution is controlled by the frequency and duration of inundation, which is principally a function of tidal elevation (e.g. Horton and Edwards, 2006; Scott and Medioli, 1978). Foraminifera are abundant in salt marshes where they form assemblages occupying narrow elevational ranges making them suitable for quantitative and precise PME reconstructions. Bulk sediment geochemistry can also be employed as a sea-level indicator. In regions where salt marshes are dominated by C_4 plants such as the mid-Atlantic and northeastern U.S., measured $\delta^{13}C$ values readily identify sediment of salt-marsh origin (e.g. Middleburg et al., 1997; Tanner et al., 2010; Wilson et al., 2005). RSL reconstructions also require the timing of sediment deposition to be estimated. Sediment that accumulated under low-energy conditions on salt marshes is often undisturbed and well suited to developing detailed chronologies. Radiocarbon is the principal means to date late Holocene salt-marsh sediment, but alternatives are necessary for the period since approximately 1650AD because of a plateau on the calibration curve (e.g. Reimer et al., 2011). Age-depth models developed from composite chronologies incorporating radiocarbon dates and age markers of pollution and land-use change enable RSL to be reconstructed with the multi-decadal precision necessary to describe small (decimeter) RSL changes (e.g. Marshall et al., 2007). The resulting RSL reconstructions filter out short-lived (annual to decadal) sea-level variability because of the time-averaging effect of sedimentation and sampling. The resulting records are analyzed using numerical tools to identify and quantify the timing and magnitude of persistent (decadal to centennial) phases of sea-level evolution.

Relative sea-level changes in New Jersey over the past ~2500 years were reconstructed to determine how and when persistent sea-level trends deviated from background rates. Reconstructions were developed from salt-marsh sediment at two sites (Leeds Point in the Edwin Forsythe National Wildlife Refuge and at Cape May Courthouse; Figure 1) using foraminifera and stable carbon isotopes ($\delta^{13}C$) as sea-level indicators and age-depth models constrained by composite chronologies of radiocarbon, ^{137}Cs activity, and pollen and pollution chrono-horizons. Change point analysis identified four persistent periods of sea-level behavior during the last 2500 years that mark positive and negative departures from a linear background rate. The new reconstructions demonstrate that the rate of sea-level rise since ~1850AD exceeds any previous persistent rate in the late Holocene.

2. Study Area

The New Jersey coast from Great Bay to Cape May consists of a barrier island and lagoon system separating the mainland from the Atlantic Ocean (Figure 1). Inlets allow exchange of water between the lagoons and ocean. Great diurnal tidal ranges are smaller in the lagoons (typically 1.1m to 1.2m, but as small as 0.17m in the upper reaches of Barnegat Bay) than on the ocean side of the barrier islands (e.g. 1.4m at Atlantic City). Tidal influence extends up to 25km from the coast into bays and brackish river systems such as Great Egg Harbor River. Modeling of paleotides in New Jersey indicates that great diurnal tidal range changed very little during the late Holocene, even at the scale of coastal embayments and estuaries (Horton et al., 2013).

Modern salt marshes in the study region form extensive (often more than 1km wide) platforms with very gentle elevation gradients. Tidal flats are rare in New Jersey because the marsh front is usually a pronounced step change in elevation. Low-marsh settings between mean tide level (MTL) and mean high water (MHW) are typically vegetated by the C_4 plant *Spartina alterniflora* (tall form). The high-marsh floral zone between MHW and mean higher high water (MHHW) is vegetated by *Spartina patens*, *Distichlis spicata, and Spartina alterniflora* (short form), all of which are C_4 plants. The transition above MHHW from high salt marsh to freshwater upland is characterized by *Phragmites australis*, *Iva fructescens,* and *Baccharis halimmifolia*, all of which are C_3 plants. At sites with greater freshwater influence, *Typha augustifolia,* and *Schoenoplectus americanus* (C_3 plants) are also common (Stuckey and Gould, 2000). Salt marshes are replaced upstream by brackish marshes dominated by *Phragmites australis*, *Typha augustifolia*, *Spartina cynosuroides,* and *Schoenoplectus americanus* (Tiner, 1985). Examples of these environments are found on the Great Egg Harbor River (Figure 1).

Several distinctive assemblages of foraminifera exist of modern salt marshes in New Jersey (Kemp et al., 2012a; Kemp et al., 2013). The dominant species in low-marsh environments are *Miliammina fusca* and *Ammobaculites* spp. High-marsh environments are populated by at least five distinctive assemblages of foraminifera, including groups dominated by *Jadammina macrescens*, *Tiphotrocha comprimata*, *Trochammina inflata*, *Arenoparrella mexicana*, and *Ammoastuta inepta* (most prevalent in low-salinity settings). At some sites *Haplophragmoides manilaensis* is the dominant species in the transitional marsh zone. Foraminifera are absent from freshwater environments.

Throughout the Holocene New Jersey experienced RSL rise from eustatic rise and isostatic subsidence. RSL 8000 years before present (yrs BP) was at approximately -12m, at 5000 yrs BP it was at -9m, and at 2000 yrs BP it was at -4m (Engelhart and Horton, 2012; Horton et al., 2013; Miller et al., 2009). During the late Holocene the primary driver of RSL change in New Jersey was glacio-isostatic subsidence caused by retreat and collapse of the Laurentide Ice Sheet's forebulge at a rate of approximately 1.4mm/yr (Engelhart et al., 2009; Engelhart et al., 2011b). As RSL rose sediment deposited in back-barrier settings (including salt-marsh peat and estuarine muds) formed sedimentary archives from which RSL changes can be reconstructed (Daddario, 1961; Meyerson, 1972; Psuty, 1986). Instrumental measurements of RSL in New Jersey are available since 1911AD when the Atlantic City tide gauge was installed. The Sandy Hook tide gauge began measurements in 1932AD, while the tide gauges at Cape May and Lewes (Delaware) provide data since 1966AD and 1919AD respectively. The linear rate of RSL rise (to

2012AD) is 4.10mm/yr at Atlantic City, 4.06mm/yr at Sandy Hook, 4.64mm/yr at Cape May, and 3.39mm/yr at Lewes.

The Leeds Point and Cape May Courthouse sites were selected after coring at numerous locations in southern New Jersey demonstrated that they had long and/or uninterrupted accumulations of salt-marsh sediment suitable for reconstructing late Holocene RSL. Leeds Point is located in the Edwin Forsythe National Wildlife Refuge on the west side of Great Bay (Figure 1A, B), in an area where salt marshes frequently exceed 1km in width (Ferland, 1990). Low-marsh areas bordering tidal creeks are vegetated by *Spartina alterniflora* (tall form). The expansive high salt-marsh platform is characterized by *Spartina patens* with *Distichlis spicata*. A narrow (10-20m wide) brackish zone bordering the surrounding forested upland is vegetated by *Phragmites australis* and *Typha augustifolia*. The Leeds Point salt marsh was extensively ditched in the early 20th century for mosquito control. As a result, shallow sediment at the site is unsuitable for RSL reconstruction, but deeper material is unaffected. VDatum (Yang et al., 2008) estimated the tidal range at the Leeds Point to be 1.11m.

Cape May Courthouse is located on the Cape May peninsular (Figure 1a, c). Vegetation at the site includes *Spartina alterniflora* (tall form) along the main tidal channel and smaller creeks, a high-salt marsh community of *Spartina patens* with *Distichlis spicata*, and a water-logged brackish environment marking the transition between salt marsh and upland. The dominant vegetation in this zone is *Phragmites australis* with *Typha augustifolia*, and *Schoenoplectus americanus*. A narrow, infilled valley was investigated because it showed little evidence of human modification. The sediment underlying the Cape May Courthouse site is suitable for detailed reconstruction of recent RSL changes including the historic period. VDatum (Yang et al., 2008) estimated the tidal range at Cape May Courthouse to be 1.40m.

3. Materials and Methods

3.1 Estimating Paleomarsh Elevation

At each site multiple transects of hand cores were recovered to describe the underlying stratigraphy. The cores chosen for detailed analysis are Leeds Point core 10 (LP-10) and Cape May Courthouse core 8 (CMC-8) because they included some of the thickest sequences of high salt-marsh peat. Cores for laboratory analysis were collected using a Russian-type core to prevent compaction during sampling, sealed in plastic wrap and kept refrigerated. Samples of core material (1cm thick) were sieved under running water to isolate and retain the foraminifera-bearing fraction between 63µm and 500µm. Foraminifera were counted wet under a binocular microscope and a minimum of 100 individuals were enumerated or the entire sample was counted if <100 were present. Identifications were made by comparison with modern examples from the study region (Kemp et al., 2013).

A weighted averaging transfer function with inverse deshrinking (WA-inv) was applied to assemblages of foraminifera in the LP-10 and CMC-8 cores to estimate the PME at which the sample was originally deposited. A unique (sample specific) uncertainty was generated for each sample using bootstrapping (n=10,000) that represents an approximately 1σ confidence interval for PME. This transfer function was developed (and described) by Kemp et al. (2013) from 175 modern samples of foraminifera compiled from 12 salt marshes in southern New Jersey (including Leeds Point and Cape May Courthouse) representing a range of physiographic settings (Figure 1a). Transfer function performance was assessed using seven tests and indicated that PME could be reconstructed with an estimated uncertainty of ±14% of great diurnal tidal range. Leave-one-site-out cross validation indicated that spatial autocorrelation caused by sampling along transects was negligible (Kemp et al., 2013). Core assemblages were analyzed after square-root transformation of population data. All taxa were retained and used in estimating PME. Reconstructions of PME from the transfer function are in standardized water level index (SWLI) units, which was used to combine modern assemblage data from sites with different tidal ranges (Horton and Edwards, 2006). A value of 0 corresponds to MLLW and 100 to MHHW.

To investigate the ecological plausibility of these reconstructions, dissimilarity between assemblages of foraminifera in core material and their closest modern counterpart was calculated using the Bray-Curtis metric. Thresholds for assessing the degree of analogy were established from pairwise analysis of the modern dataset (Kemp et al., 2013). Distances within the lower 20% of dissimilarity between modern samples were treated as having acceptable analogues, within 10% as having good analogues, and within 2% as having very strong analogues. To assess how well the transfer function fits observations of elevation, goodness-of-fit statistics were calculated for core samples by passively fitting them into a constrained ordination (canonical correspondence analysis; CCA) of the modern dataset with tidal elevation as the only constraint following the approach of Simpson and Hall (2012). The squared residual length between core samples and their fitted positions on the first constrained axis was compared to residual differences in the modern dataset. Thresholds at 90% (weak), 95% (poor), and 99% (very poor) were established from the modern dataset for progressively worse fits to tidal elevation. These two analyses were conducted on square root transformed population data using the analogue package (v.0.8-2; Simpson, 2007) for R. They represent different and independent criteria for evaluating reconstructions from transfer functions, it is possible to have a close modern analogue, but a poor fit and vice versa (Birks, 1998). Samples exceeding the 20% dissimilarity threshold and the 95% goodness-of-fit threshold were excluded from the RSL reconstruction.

The measurement of stable carbon isotopes in core material (1cm thick bulk sediment) used the same sample-preparation method and instrument as the measurements made on modern salt-marsh sediment from New Jersey (Kemp et al., 2012c). Reported $\delta^{13}C$ values were calculated to the Vienna Pee Dee Belemnite scale (VPDB; ‰). Comparisons to standards were always within 0.1‰ and confirm that measured $\delta^{13}C$ values are accurate. Replicate analysis of well-mixed samples indicated precision of $\pm <0.1$‰ for $\delta^{13}C$ measurements (1σ). Analysis of modern salt-marsh sediment in New Jersey demonstrated that bulk sediment with $\delta^{13}C$ values more depleted than -22.0‰ formed above MHHW, while values less depleted than -18.9‰ were associated with low and high salt-marsh environments situated between MTL and MHHW (Kemp et al., 2012c). This distinction results from the photosynthetic pathways of C_3 and C_4 plants. On the mid-Atlantic and northeastern coasts of the United States (including New Jersey) elevations below MHHW are vegetated by C_4 plants (e.g. *Spartina* spp., *Distichlis spicata*), while elevations above MHHW are vegetated by C_3 plants (e.g. *Phragmites australis*, *Iva fructescens*). Since the dominant input to salt-marsh sediment is *in-situ* vegetation (Chmura and Aharon, 1995), $\delta^{13}C$ values measured in bulk sediment provide a simple and reliable means to determine if a sample was deposited above or below the MHHW tidal datum (e.g. Johnson et al., 2007; Kemp et al., 2012c). All salt marshes receive a contribution to bulk sediment from allocthonous organic matter (e.g. marine phytoplankton), although it is usually a minor component of measured $\delta^{13}C$ values (Lamb et al., 2006) and insufficient in most cases to influence paleoenvironmental interpretation. The difference between living plant material and bulk surface sediment similar in composition to the New Jersey cores is <7‰ (Benner et al., 1991; Goñi and Thomas, 2000) and insufficient to cause mis-interpretation of dominance by C_3 or C_4 plants (e.g. Benner et al., 1987; Ember et al., 1987; Fogel et al., 1989). Empirical results indicate that there is little post-burial modification of bulk sediment $\delta^{13}C$ values (Byrne et al., 2001; Malamud-Roam and Ingram, 2004). Indeed, an investigation of $\delta^{13}C$ values in plants, surface sediment, and buried sediment at the Leeds Point site concluded that no systematic, post-burial shift could be discerned for bulk sediment derived from salt-marsh plants (Kemp et al., 2012c). Therefore $\delta^{13}C$

values are a robust tool for distinguishing between bulk sediment that accumulated in environments dominated by C_3 or C_4 plants. Identification of extant surface vegetation to the species level would require complementary biogeochemical techniques such as molecular markers and isotopic discrimination (carbon and other elements) within structural compounds such as lignin or cellulose (e.g. Middleburg et al., 1997; Tanner et al., 2010; Vane et al., 2013).

To utilize all available palaeoenvironmental information, PME was estimated for core samples by combining results from the foraminiferal transfer function and downcore measurements of $\delta^{13}C$. The range of transfer function reconstructions was restricted to elevations in agreement with those estimated from measured $\delta^{13}C$ values. The restricted ranges were treated as having uniform probability distributions in subsequent analysis. PME was therefore reconstructed in one of three ways:

i) For samples with a $\delta^{13}C$ value more depleted than -22‰, the transfer function estimate was trimmed to retain only the range above MHHW (SWLI>100) because C_3 plants were the dominant type of vegetation;

ii) For samples with a $\delta^{13}C$ value less depleted than -18.9‰, the transfer function estimate was trimmed to retain only the range below MHHW (SWLI<100) because C_4 plants were the dominant type of vegetation;

iii) For samples with intermediate $\delta^{13}C$ values (-22.0‰ to -18.9‰), and/or transfer function estimates that did not encompass MHHW, the full range of the original transfer function was retained because it was not possible to reliably determine if C_3 or C_4 plant species were the dominant type of vegetation.

3.2 Dating and Age-Depth Modeling

Radiocarbon dating was performed on identifiable plant macrofossils found in growth position in the cores. Macrofossils were separated from the sediment matrix and cleaned under a microscope to remove contaminating material including adhered sediment particles and in-growing younger roots. The cleaned samples were oven-dried at 45ºC and submitted to the National Ocean Science Accelerator Mass Spectrometry (NOSAMS) facility for dating. At NOSAMS, all samples underwent standard acid-base-acid pretreatment. Reported radiocarbon ages and uncertainties (Table 1) were calibrated using the Intcal09 dataset (Reimer et al., 2011). Measured $\delta^{13}C$ values for radiocarbon dates are from an aliquot of

CO_2 collected during sample combustion and were used to correct for natural fractionation of carbon isotopes.

Activity of ^{137}Cs in CMC-8 was measured at the Yale University Environmental Science Center by gamma spectroscopy. Peak ^{137}Cs activity in core material identifies sediment deposited around 1963AD when above ground testing of nuclear weapons was at its maximum (Warneke et al., 2002). Concentrations of elements (Cu, Pb, Zn, Cd, and Ni) and isotopic ratios (^{206}Pb:^{207}Pb) were measured at the British Geological Survey Environmental Science Centre to establish the timing of recent sediment deposition in CMC-8. Bulk samples (1cm thick) were prepared in an identical manner to that previously described by Vane et al. (2011) and analyzed using a quadropole ICP-MS instrument (Agilent 7500c) operated under the conditions specified in Kemp et al. (2012b). Concentrations were not normalized by grain size because in salt-marsh environments, heavy metal pollutants are more strongly associated with organic content (Vane et al., 2009), which was high (30-40% by weight) and relatively uniform in the upper section of core CMC8. Normalization is an appropriate step for comparing concentrations among sites, but it was not necessary for identifying trends within a single core. Downcore trends in absolute elemental concentration and their stratigraphic position were matched to features of historic production and consumption. Interpretation of the Pb and ^{206}Pb:^{207}Pb profiles in CMC-8 followed the approaches described in similar studies (e.g. Gobeil et al., 2013; Kemp et al., 2012b; Lima et al., 2005). In addition, the downcore Zn profile was compared to regional production records to recognize the onset (1880-1900AD) and peak (1943-1969AD) of industrial output (Bleiwas and DiFrancesco, 2010). National production records from the United States Geological Survey Minerals Yearbook also enabled recognition of peaks in Cd (1956-1969AD) and Ni (1950-1980AD; 1992-2002AD) and the onset of Cu pollution (1890-1910AD). Changes in production and consumption were assumed to have caused a corresponding change in elemental emissions that were transported through the atmosphere by constant prevailing wind patterns and deposited on the salt-marsh surface within a few years (Bollhöfer and Rosman, 2001; Graney et al., 1995) and without isotopic fractionation (Ault et al., 1970). Since emissions per unit of production or consumption changed through time, trends rather than absolute values were the basis for recognizing these features in core CMC8. Comparison of independent chronologies developed using markers of industrial pollution and radiometric decay of ^{210}Pb activity elsewhere in New Jersey indicated that heavy metal pollution is synchronous with industrial activity within the age and sample thickness uncertainties assigned to each marker (Kemp et al., 2012b).

Palynomorphs (pollen and fern spores) were isolated from 1cm thick sediment slices of core CMC-8 using standard palynological preparation techniques (Traverse, 2007). At least 300 pollen grains and spores were counted from each sample to determine percent abundance of palynomorphs. The rise of *Ambrosia* in southern New Jersey was estimated to be 1710AD ± 50 years based on histories of European arrival and colonization of the region; the areas around Leeds Point and Cape May Courthouse were first settled between 1695AD and 1725AD (Wacker, 1975; Wacker and Clemens, 1994).

Discrete dated samples were used to generate separate accumulation histories for LP-10 and CMC-8 using the Bchron package (v.3.1.5; Haslett and Parnell, 2008; Parnell et al., 2008) executed in R. Excess ^{210}Pb was measured in CMC-8, but it was excluded from the age-depth model because the age estimates for individual samples would be treated as independent by Bchron. Since ^{210}Pb accumulation histories are modeled, the resulting suite of down core age estimates are not independent of one another and would cause the Bchron age-depth model to be weighted (and unfairly biased) toward ^{210}Pb results. Chrono horizons associated with ^{137}Cs, pollution markers, and pollen were treated as having uniform probability distributions. Bchron utilized a Bayesian approach to produce an age-depth model for both cores. From a suite of 200,000 iterations the age-depth models provides an estimate of age with a 95% confidence interval for every 1cm thick interval in the cores. This age estimate and uncertainty was applied to all samples with reconstructed PME.

3.3 Reconstructing Relative Sea Level and Identifying Persistent Sea-Level Trends

Relative sea level was reconstructed by subtracting the estimated PME for each sample from the measured elevation at which the sample was recovered (depth in core), where both values were expressed relative to mean tide level (MTL). Core top elevations were established using real time kinematic (RTK) satellite navigation with conversion from orthometric to tidal datums using VDatum (v2.3.5, New Jersey coastal embayment dataset v1). Core LP-10 is at 0.56m MTL and core CMC-8 is at 0.53m MTL. The vertical uncertainty of the reconstruction is the range from the transfer function that was amended by $\delta^{13}C$ values. The age (with associated range) of each core sample was taken directly from the age-depth model. RSL data are presented as boxes, where the height represents sea-level error and the width is age error. RSL data are provided in appendix A.

Following adjustment for the estimated rate of land subsidence in New Jersey, the independent reconstructions from Leeds Point and Cape May Courthouse were combined into a single dataset and reordered by age. The combined record has the advantage over analyzing two individual records of spanning all of the last 2500 years. Change point analysis of this dataset identified periods of persistent sea-level variability in New Jersey during the late Holocene and estimated the timing of change points and the rate of sea-level rise between them with 95% confidence. Proxy reconstructions are characterized by age and sea-level errors that are unique to each sample and an uneven distribution of samples in time. Simple linear regression is therefore an unsuitable method of analysis since it assumes that the explanatory variable (x, in this case age) is fixed and known. An extension of the error-in-variables (EIV) model is applied to proxy reconstructions because it accounts for both age and sea-level uncertainties (Spiegelhalter et al., 2002).

The simplest EIV model can be written as

$$y_i = \alpha + \beta \mu_{xi} + \varepsilon_i$$

Where y_i is sea level for the ith observation, α is the intercept, β is the rate of sea-level change, and μ_{xi} is the unknown age for the ith observation. Since ages in paleoenvironmental reconstructions have uncertainty it is treated as an unknown random variable to be estimated. The term ε_i is the model error for the ith observation which incorporates the uncertainty for each sea-level reconstruction which is fixed and known and also an unknown error which was not included in the measurement error. Therefore

$\varepsilon_i \sim N\left(0, \sigma_{yi}^2 + \tau_y\right)$, and $x_i = \mu_{xi} + \delta_i$, and $\delta_i \sim N(0, \sigma_{xi}^2)$.

The terms σ^2_{yi} and σ^2_{xi} are the variances of sea level and age respectively. The variance parameter (τ_y) represents overall variation in the dataset. The model assumes that x_i and y_i follow the bivariate normal distribution shown below where x_i is sample age and y_i is reconstructed sea level for samples i to n.

$$\begin{pmatrix} x_i \\ y_i \end{pmatrix} \sim N\left(\begin{pmatrix} \mu_{xi} \\ \mu_{yi} \end{pmatrix}, \begin{pmatrix} \sigma^2{}_{xi} \sigma_{xiyi} \\ \sigma_{xiyi} \sigma^2{}_{yi} \end{pmatrix}\right)$$

With a single change point it is assumed that the data follow one EIV model before the change point, where $\mu_{yi} \sim N(\alpha + \beta_1 (x_i - x_{change}), \tau_y)$, and another EIV model afterward, where $\mu_{yi} \sim N(\alpha + \beta_2 (x_i - x_{change}), \tau_y)$. The parameter x_{change} represents the age at which the sea-level rate changes significantly, and the parameters β_1 and β_2 are the rate before and after the change point respectively. For the New Jersey sea-level reconstruction the model was extended to include one to four change points. The model that best describes the data was selected using the deviance information criterion (DIC; Spiegelhalter et al., 2002) which is a Bayesian method for model comparison, where the posterior distribution was obtained by Markov Chain Monte Carlo simulation. Deviance is a measure of distance between the data (reconstructed sea level) and model predictions. More complex models will almost always have lower deviance and are consequently penalized relative to the number of unconstrained parameters in the model. DIC accounts for both mean deviance and also complexity to ensure that model selection is fair and unbiased. Models with lower are preferable to those with larger DIC. Since the data are corrected for the contribution of land-level changes, the covariance matrix for the EIV model accounts for the distortion of data points from rectangles to parallelograms and the angle of the parallelogram (i.e. the rate of land-level change).

4. Results

4.1 Foraminifera and $\delta^{13}C$ values in cores from Leeds Point (LP-10) and Cape May Courthouse (CMC-8)

To establish the environment and elevation of sediment deposition, foraminifera were counted in core samples positioned at regular intervals, dated levels, and to capture transitions between assemblage types and stratigraphic units. The lowest occurrence of foraminifera in LP-10 was at 3.95m (Figure 2). Between 3.95m and 2.85m the most common foraminifera was *Jadammina macrescens* that occurred with *Tiphotrocha comprimata* and *Trochammina inflata*. The interval between 3.13m and 3.00m was characterized by an unusually high abundance of *Miliammina petila* (24-60%), while the low-marsh species *Miliammina fusca* was common (>20%) from 2.82m to 2.95m. *Trochammina inflata* was the dominant species of foraminifera from 2.82m to 1.85m. Foraminifera were absent between 1.85m and 1.73m The uppermost section of LP-10 (1.73m to 1.20m) was comprised of a near mono-specific assemblage of *Jadammina macrescens*. Foraminifera were present in the top 1.20m of LP-10, but were not analyzed in detail because this material was unsuitable for sea-level reconstruction due to human modification. Foraminifera throughout core LP-10 indicate deposition in a high salt-marsh environment.

Measurements of $\delta^{13}C$ values were made on bulk sediment in LP-10 at regularly spaced intervals to establish the botanical and environmental origin of core samples. At depths between 4.20m and 3.31m $\delta^{13}C$ values varied from -27.0‰ to -22.2‰ (Figure 2), which is characteristic of an environment dominated by C_3 plants such as those in the transition between salt marsh and freshwater upland communities. This sedimentary unit was a black, amorphous organic unit. The interval between 3.26m and 2.86m included some $\delta^{13}C$ values (-21.4‰ to -19.1‰) that are intermediate between those of modern C_3 and C_4 plants. Measured $\delta^{13}C$ values in the upper 2.81m of LP-10 varied from -16.8‰ to -13.1‰ and were typical of a salt-marsh environment vegetated by C_4 plants. These $\delta^{13}C$ values indicate that the section of LP-10 that was devoid of foraminifera (1.85m to 1.73m) formed in a salt-marsh environment.

Foraminifera were present in core CMC-8 to a depth of 2.22m, but below 1.72m there were few individuals and these sparse assemblages were not considered suitable for quantitative analysis (Figure 3). From 1.72m to 1.29m, assemblages were largely composed of *Jadammina macrescens* and *Trochammina inflata*. Foraminifera were absent between 1.25m and 1.12m. The dominant species from 1.10m to 0.33m was *Jadammina macrescens*, while samples from 0.31m to 0.05m had assemblages of *Trochammina inflata*, *Tiphotrocha comprimata* and *Jadammina macrescens*. These assemblages demonstrate that core CMC-8 accumulated in a high salt-marsh environment. The two uppermost samples (0.03m and 0.05m) had an assemblage that included 17% and 21% *Miliammina fusca* respectively. In core CMC-8, bulk sediment between 2.58m and 1.85m had $\delta^{13}C$ values between -28.6‰ and -22.1‰ (Figure 3), which is typical of an environment dominated by organic inputs from C_3 plants. This sedimentary unit was a black, amorphous organic unit. The uppermost 1.78m of the core included samples with $\delta^{13}C$ values from -18.9‰ to -13.1‰, which fall within the range of modern salt marshes dominated by C_4 plants in New Jersey. This indicates that sediment in the interval devoid of foraminifera (1.25m to 1.12m) formed in a salt marsh. A single sample at 1.81m had an intermediate value of -20.3‰.

4.2 Transfer function application and evaluation

To reconstruct paleomarsh elevation (PME), the regional weighted-averaging transfer function with inverse deshrinking (WA-inv) of Kemp et al. (2013) was applied to assemblages of foraminifera enumerated from cores LP-10 and CMC-8 (Figures 2 and 3). The transfer function estimated PME and an uncertainty (in SWLI units) derived by bootstrapping that is unique to each sample. In LP-10, transfer function estimates of PME ranged from 54 to 111 SWLI units (average 95) with an average uncertainty of ±14 SWLI units (equating to ±0.15m at this site). Samples with high abundances of *Miliammina petila* between 3.10m and 3.00m had slightly above average reconstructed PMEs (average 104 SWLI units), while the eight samples in which the low-marsh foraminifera *Miliammina fusca* made up more than 20%

of the assemblage (2.98m to 2.82m) had correspondingly lower PME (average 75 SWLI units). PME estimated by the transfer function for samples in CMC-8 reflects the dominance of high-marsh species of foraminifera (*Jadammina macrescens, Trochammina inflata* and *Tiphotrocha comprimata*) throughout the core. The average PME was 97 SWLI units with an uncertainty of ±14 SWLI units (equating to ±0.20m at this site). The two samples near the top of the core with increased *Miliammina fusca* formed at a slightly lower PME (86 to 88 SWLI).

To judge ecological plausibility of transfer function results, the measured dissimilarity between core samples and their closest modern counterpart was compared to thresholds established by pairwise comparison of the modern training set. In LP-10, 74 samples were within the 20th percentile threshold for an acceptable modern analogue that was established from pairwise analysis of the training set (Figure 2). Twenty two samples exceeded this threshold, including most samples above 1.75m that were comprised of near-monospecific assemblages of *Jadammina macrescens*. These samples lacked a modern analogue because *Jadammina macrescens* had a maximum abundance of 62% in the modern training set. The samples exceeding the 20th percentile threshold between 3.03m and 3.25m included abundances of *Miliammina petila* that exceed its maximum contribution to any modern sample (19%). In CMC-8, seven samples had a minimum dissimilarity exceeding the 20th percentile because they included abundances of *Jadammina macrescens* greater than any sample in the modern training set (Figure 3).

The validity of elevation reconstructions was judged using goodness-of-fit statistics where core samples were positioned passively on the ordination of modern samples and residual fits were compared to thresholds for weak (90%), poor (95%), or very poor (99%) fits. In LP-10, 23 samples exceeded the 95% threshold established for a poor or very poor fit (Figure 2). These samples were associated with the interval where *Miliammina petila* was abundant and also in the uppermost 1.72m where *Jadammina macrescens* formed near mono-specific assemblages. In most cases, samples with large residual lengths were also dissimilar to modern samples in their faunal composition. In CMC-8, three samples surpassed the 95% threshold for a poor or very poor fit (Figure 3).

4.3 Core chronologies

In LP-10, 21 radiocarbon dates on identifiable plant macrofossils show that accumulation of organic sediment began at approximately 600 BC (Figure 4; Table 1). The Bchron age-depth model was developed using all 21 radiocarbon dates and estimated the age of each 1cm thick interval in LP-10 with a unique uncertainty that ranged from ±17 years to ±113 years (average of ±50 years). From the lowest dated level (3.93m; approximately 580BC) to the radiocarbon date at 3.14m (286AD), the average rate of sediment accumulation was 0.9mm/yr. From 286AD to 1344AD, the average rate of sediment accumulation in LP-10 was 1.6mm/yr and from 1344AD to 1570AD it averaged 0.8mm/yr.

To provide a decadal chronology for the period since ~1650AD that is affected by the radiocarbon plateau, the upper 0.70m of core CMC-8 was dated by identifying chronohorizons from changes in pollen (*Ambrosia*), concentrations of Pb, Zn, Cu, Cd, and Ni, ^{137}Cs activity, and shifts in the isotopic ratio of ^{206}Pb:^{207}Pb (Figure 5). These downcore changes were related to historic events such as widespread land clearance by European settlers and trends in national and regional industrial production. In addition to these age estimates, 13 radiocarbon dates constrain the timing of sediment deposition from 0.76m to 2.08m (Figure 6). Accumulation of organic material at the core site began at around 700AD and continued without interruption to the present day. All chronological data provided constrains for the Bchron (Parnell et al., 2008) age-depth model that estimated the age of each 1cm interval in the core with errors ranging from ±1.5 years to ±58 years (average ±28.5 years). The average rate of sediment accumulation in CMC-8 between 700AD and 1850AD was approximately 1.3mm/yr, after which it increased to 3.9mm/yr (Figure 6).

5. Sea Level Change in New Jersey

The New Jersey RSL reconstruction is represented by boxes that incorporate sea-level and age uncertainty (Figure 7). Core samples that lacked a modern analogue (>20% threshold for dissimilarity) and had a poor or very poor fit to tidal elevation (>95% threshold for goodness-of-fit) were excluded. The Leeds Point and Cape May Courthouse sites experienced sediment accumulation for the period under consideration as a result of RSL rise. RSL in New Jersey was -4.20m at approximately 500BC and rose to -0.70m at around 1850AD (Figure 7). Agreement between the RSL reconstructions from Cape May Courthouse and Leeds Point between 970AD and 1460AD indicates that local-scale processes were not the dominant drivers of RSL in New Jersey, at least for that shared interval. The RSL reconstruction lies within the uncertainties of basal reconstructions compiled for New Jersey (Figure 7a) indicating a lack of detectable compaction. Furthermore, the overlap and coherence of the reconstructions from Leeds Point and Cape May Courthouse which have different sediment thicknesses and compositions indicates that compaction did not make a significant contribution to reconstructed RSL trends, likely because the saturated, low density nature of salt-marsh peat makes it resistant to compaction (e.g. Brain et al., 2012). Similarly, annual RSL measurements from tide gauges at Atlantic City, Sandy Hook, Cape May, and Lewes display a high degree of coherence, demonstrating that local processes are not the dominant drivers of historical RSL change in New Jersey (Figure 8a). A regional tide-gauge record generated by averaging the four gauges shows approximately 0.37m of RSL rise in New Jersey since 1911AD at an average rate of 4.03mm/yr (Figure 8b). During the 20th century, RSL was reconstructed to be approximately 0.4m. The averaged tide-gauge measurements lie within the age and vertical uncertainties of the RSL reconstruction and give confidence that the reconstruction is an accurate representation of long-term, persistent RSL changes in New Jersey.

Measurements and reconstructions of RSL are the net result of multiple processes that often act simultaneously. To allow comparisons among regions and to identify climate-related sea-level trends, it is necessary to estimate and remove the contribution made by land-level changes. The principal mechanism for regional land-level change in coastal New Jersey during the late Holocene was GIA from collapse and retreat of the Laurentide Ice Sheet's proglacial forebulge (Engelhart et al., 2011b). The ICE6G-VM5b Earth-Ice model predicts RSL being 2.13m below present at 2000 yrs BP at Cape May Courthouse and Leeds Point (Engelhart et al., 2011b). Eustatic input ceases at 4000 yrs BP in this model, since when all RSL changes (1.1mm/yr) are attributed to GIA and associated processes such as redistribution of water in response to changes in the geoid. The total contribution of land-level change also includes tectonic processes and regional sediment consolidation. Total land-level change was estimated from a regional compilation of basal RSL reconstructions (Shennan et al., 2012). This approach fits a linear regression to late Holocene, basal, sea-level index points (up to 1900AD) and like the Earth-Ice model assumes there was no eustatic contribution, meaning that the RSL trend approximates land-level changes (Engelhart et al., 2009). This approach captures land-level changes caused by processes other than GIA. For New Jersey, the estimated rate of land-level change is subsidence of 1.4mm/yr (Engelhart et al., 2011b). The difference (0.3mm/yr) in rates estimated from the Earth-Ice model and database of sea-level index points could be from land-level change caused by non-GIA processes or a misfit in model parameters.

It is widely assumed that late Holocene sea level was stable at multi-decadal to multi-centennial timescales until the onset of modern rates of rise in the late 19th or early 20th century (Bindoff et al., 2007; Church et al., 2008; Cronin, 2012). The annual to decadal variability that is apparent in tide-gauge records must also have characterized the late Holocene. Given the attribution of 20th century sea-level rise to global climate change (e.g. Rahmstorf, 2007), it is reasonable to expect phases of sea-level behavior within the late Holocene related to known phases of warmer (e.g. Medieval Climate Anomaly) and cooler (e.g. Little Ice Age) temperatures. To challenge the assumption of stability it is necessary to reconstruct sea level through the full late Holocene period with accuracy and precision that enables confident identification of relatively small and relatively short lived sea-level changes. Therefore the New Jersey reconstruction represents a suitable dataset for identifying regional departures from late Holocene stability after correction for land-level changes. After subtracting 1.4mm/yr of land-level change from the RSL reconstructions three change points were identified using the EIV model (Figure 9). Models with fewer, or more than, three change points were inferior because they had larger DIC values (Table 2). The three change points therefore define four periods of persistent (centennial) sea-level trends. From at least 500BC to 250AD sea level fell at a mean rate of 0.11mm/yr. The second period saw sea level rise at a mean rate of 0.62mm/yr from 250AD to 733AD. Between 733AD and 1850AD sea level fell at a mean rate of 0.12mm/yr. Since 1850AD the reconstructed rate of sea-level rise was 3.1mm/yr. Late Holocene sea-level changes in New Jersey include distinct positive and negative departures from background rates and demonstrate that the assumption of sea-level stability (in this region at least) is unjustified.

The most prominent feature in the New Jersey sea-level reconstruction is the inflection that marks the initiation of modern rates of sea-level rise between 1830AD and 1873AD (Table 2; Figure 9a). Using a global compilation of tide-gauge records (Church and White (2006); 2011) recognized an increase in the rate of sea-level rise at around 1930AD, but concluded that the primary change from background to modern rates of rise likely occurred prior to 1870AD. Therefore the onset of modern rates of sea-level rise pre-dates all tide gauges in New Jersey and almost all globally. Based on the limited number of pre-1870AD gauges, Jevrejeva et al. (2008) developed a global tide-gauge record since 1700AD and concluded that accelerated sea-level rise may have begun in the late 18th century. Sea-level reconstructions from salt-marsh sediment address the limited duration of instrumental data and estimate when modern rates of rise began (Barlow et al., 2013). In North Carolina, change point analysis identified the increase in rate as occurring between 1865AD and 1892AD (Kemp et al., 2011). In Connecticut, the change was identified in the second half of the 19th century from the difference between reconstructed background rates and modern rates of rise measured by tide gauges (Donnelly et al., 2004). The onset of modern sea-level rise in New Jersey is broadly synchronous with similar studies from the U.S. Atlantic coast. From a salt-marsh reconstruction in Nova Scotia, the transition to modern rates of rise was subjectively identified between 1930AD and 1940AD from the intersection of two linear regressions without formal consideration of temporal and vertical uncertainties in the sea-level reconstruction (Gehrels et al., 2005; Gehrels and Woodworth, 2012). Using the same approach, sea-level reconstructions from the southern hemisphere (Tasmania and New Zealand) placed the inflection in the rate of sea-level rise between 1895AD and 1925AD (Gehrels et al., 2012; Gehrels et al., 2008; Gehrels and Woodworth, 2012). This difference in timings may reflect a real global pattern or be a consequence of the methods used to estimate timing and rates.

The reconstructed rate of sea-level rise in New Jersey since the inflection between 1865AD and 1892AD is 3.1mm/yr (95% confidence interval of 2.8mm/yr to 3.5mm/yr; Figure 9a, Table 2) and is unprecedented for at least 2500 years. This rate exceeds the global average estimated for the 20th century of 1.7mm/yr (Church and White, 2006; Church and White, 2011) as well as the U.S. Atlantic average of 1.8mm/yr (Engelhart et al., 2009). It also exceeds the reconstructed rate for this period from regions to the south (North Carolina, 2.1mm/yr) and north of New Jersey (Nova Scotia, 1.4mm/yr) on the Atlantic coast of North America. Processes causing exaggerated rates of land subsidence such as ground water withdrawal are often invoked for explaining the high rate of sea-level rise at the New Jersey coast (Davis, 1987; Sun et al., 1999). Local and sub-regional scale factors such as these are not captured by the database of sea-level index points used to estimate land-level change, particularly if the process(es) began in the historical period (e.g. ground-water pumping). However, the high degree of coherence among New Jersey tide gauges (Figure 8a) suggests that a regional rather than local process is the driving mechanism. Regional land-level changes in addition to GIA (e.g. long term subsidence of the coastal plain) cannot be invoked as the cause of the high rate of sea-level rise since these are inherently included in the regional database of sea-level index points. Similarly a methodological effect (e.g. change in dating methods) cannot be invoked since the reconstructions are in agreement with regional tide-gauge data (Figure 8) and the same approach used elsewhere (e.g. Nova Scotia, North Carolina) did not generate such high rates of rise. Therefore the high rate of regional sea-level rise in New Jersey since ~1850AD is attributed to oceanographic, ocean mass, or ocean volume effects. New Jersey is located in the region between Cape Hatteras and Cape Cod where tide gauges recorded rates of rise considerably greater than the global mean during the 20th century (Boon, 2012; Sallenger et al., 2012). Model results predict that changes in ocean circulation in the 21st century would result in excess sea-level rise (up to ~0.3m) along the northeastern coast of the United States (Yin et al., 2009). The high rate of sea-level rise reconstructed in New Jersey is in agreement with instrumental measurements and indicates that regional processes began to cause this spatial pattern of excess sea-level rise around 1850AD.

Prior to the onset of increased rates of sea-level rise around 1850AD, New Jersey experienced three additional periods of persistent sea-level trends (Figure 9a). Phases of late Holocene sea-level rise representing departures from a linear trend have also been reconstructed in Connecticut (Thomas and Varekamp, 1991; van de Plassche, 2000; van de Plassche et al., 1998), but in some cases were reinterpreted as sedimentary features caused by erosion of salt marshes during hurricanes or large storms followed by rapid infilling of accommodation space (van de Plassche et al., 2006). Salt-marsh reconstructions from Massachusetts (Kemp et al., 2011), Maine (Gehrels, 2000), and the Gulf of Mexico (González and Törnqvist, 2009) show evidence of late Holocene sea-level changes but lack the resolution necessary to definitively identify these features within the limitations of age and sea-level uncertainties. The late Holocene reconstruction from North Carolina included four phases of sea-level change after adjustment for land-level changes that could not be accommodated by a linear rate of change (Kemp et al., 2011). To ensure compatibility with the New Jersey reconstruction, the same error-in-variables change point model was applied to the North Carolina dataset. A model with three change points best described the reconstruction as evidenced by the lowest DIC, resulting in four persistent sea-level trends that are slightly different to those reported in (Kemp et al., 2011). In North Carolina, sea level was stable from at least 100BC to 968AD. It then increased for ~400 years at a rate of 0.5 mm/yr, followed by a further period of stable, or slightly falling, sea level until the late 19th century. After 1877AD, sea level rose at an average rate of 2.0 mm/yr (Figure 9b). These changes were attributed to climate variability, with sea-level rise being caused by Medieval warmth, stable or slightly falling sea level as a consequence of the cooler Little Ice Age, and the sharp rise since the end of the 19th century driven by contemporary warming (Kemp et al., 2011). With the exception of the historic onset of more rapid sea-level rise (1862-1873AD is the period of mutual overlap) these phases are asynchronous, with changes in New Jersey predating those in North Carolina.

Gehrels et al. (2005) recognized that calibrating radiocarbon ages from salt marshes can generate apparent sea-level changes that are artifacts of calibration. Using simulated radiocarbon dates spaced at regular temporal intervals, they generated stacked calibrated ages (more rapid "sea-level rise") at times when the calibration curve is relatively flat (plateaus) and multiple calibrated ranges are generated for a single date.

Of interest to understanding the pattern of sea-level rise reconstructed in New Jersey are examples of these periods at around 800AD and 1600AD. The asynchroneity and timing of Medieval sea-level rise in New Jersey (250AD to 750AD) and North Carolina (950AD to 1375AD) indicates that these reconstructed trends are not artifacts of radiocarbon calibration. Since the two, independent, sea-level reconstructions span a similar period of time, with a similar concentration of radiocarbon dates, they would be expected to experience simultaneous changes in sea level if they were an artifact of calibration. Therefore radiocarbon calibration is unlikely to be the cause of the reconstructed sea-level rise and a physical explanation must be sought. Alternatively, the differences between the North Carolina and New Jersey could potentially be explained by relaxing the assumption of constant, linear rates of vertical land-level change to allow a more complex spatio-temporal contribution to RSL from crustal motion. However, Earth-Ice models suggest that a linear rate of GIA is appropriate for the time scale under consideration and this assertion is supported by compilations of RSL contributions from the U.S. Atlantic coast (e.g. Engelhart et al., 2011a).

Although the first period of sea-level rise in New Jersey and North Carolina was asynchronous in timing, the rates of change (following correction of the land-level contribution) are similar. In both regions the rate of rise was 0.5mm/yr to 0.6mm/yr, preceded by an interval of stable or slightly falling sea level (0.0 to -0.1mm/yr) and followed by a second period of stable sea level (Figure 9). This agreement could indicate a common driving mechanism with a spatial lag time. The rise in North Carolina was attributed to a warmer global climate during the Medieval Climate Anomaly (Kemp et al., 2011). The reconstruction from New Jersey suggests a complex response of sea level to paleo-climate change that results in spatial variability. On decadal timescales instrumental measurements of historic sea level indicate that steric expansion (e.g. Cazenave and Llovel, 2010) and ocean circulation (e.g. Bingham and Hughes, 2009; Ezer et al., 2013; Kienert and Rahmstorf, 2012) cause spatial variability in sea level along the U.S. Atlantic coast. It is currently unclear if these processes can be invoked as a plausible mechanism for explaining spatial variability on centennial timescales. However, the New Jersey and North Carolina reconstructions are currently the only two studies to cover the entire late Holocene with the resolution needed to identify this level of variability and test hypotheses about mechanisms for pre instrumental sea-level changes. Reconstructions from other locations that encompass this interval of sea-level variability rather than focusing exclusively on the transition to modern rates of rise are needed to elucidate a coherent evolution of late Holocene sea-level change. Understanding the origin and causes of these phases of late Holocene sea-level change will help to predict the future response of sea level to projected changes in global climate.

6. Conclusions

Relative sea level (RSL) was reconstructed at two sites in New Jersey from sequences of salt-marsh sediment. A multi-proxy approach combining a transfer function trained on the modern distribution of foraminifera and bulk sediment $\delta^{13}C$ values as sea-level indicators estimated the elevation at which samples formed in one of three ways. (i) For samples with a $\delta^{13}C$ value more depleted than -22‰, the transfer function estimate was trimmed to retain only the range above MHHW; (ii) For samples with a $\delta^{13}C$ value less depleted than -18.9‰, the transfer function estimate was trimmed to retain only the range below MHHW; and (iii) For samples with intermediate $\delta^{13}C$ values (-22.0‰ to -18.9‰), and/or transfer function estimates that did not encompass MHHW, the full range of the original transfer function was retained. Sample ages were estimated using an age-depth model developed from a composite chronology of radiocarbon dates and chrono-horizons recognized by changes in elemental concentration, ^{137}Cs activity, ratios of lead isotopes and pollen abundance that were related to historical trends. The RSL reconstructions span the last 2500 years with an average vertical uncertainty of ±0.12m and average age uncertainty of ±32 years.

To test if sea level was stable during the late Holocene and identify positive and negative departures from background rates of change, an estimated rate of land subsidence (1.4 mm/yr) was removed. Change point analysis identified four periods of persistent (multi-centennial) sea-level trends in the resulting record. These deviations confirm that late Holocene sea level in New Jersey was not stable. From at least 500BC to 250AD sea level fell at 0.11mm/yr. Sea-level rose at 0.62mm/yr from 250AD to 733AD. Between 733AD and 1850AD sea level fell at 0.12mm/yr. Since 1850AD the reconstructed rate of sea-level rise was 3.1mm/yr, which is greater than any other persistent trend in at least the preceding 2500 years. The onset of modern rates of rise in the late 19th century is synchronous with reconstructions from other locations on the U.S. east coast. The modern rate of rise is in agreement with regional tide-gauge records and exceeds the global average estimate for the 20th century. The asynchroneity of Medieval sea level rise between New Jersey and North Carolina suggests that the reconstructed sea-level variability is not an artifact of radiocarbon calibration and therefore requires a physical explanation.

Acknowledgments

This work was supported by National Oceanic and Atmospheric Administration award NA11OAR4310101. Kemp thanks post-doctoral support from the Yale Climate and Energy Institute and a graduate student internship at NOSAMS that provided radiocarbon dating under the supervision of Dr. Mark Roberts. Vane publishes with permission of the director of the British Geological Survey who partially supported this work through the BGS Climate and Landscape research program. We thank the Edwin Forsythe National Wildlife Refuge (U.S. Fish and Wildlife Service) for granting access and student volunteers from the Earthwatch Student Challenge Award Program for their enthusiastic help for in fieldwork. We thank Daria Nikitina, Nicole Khan, Jessica Pilarczyk, and Andrea Hawkes for their assistance in the field and in the lab. W.R. Peltier and R. Drummond kindly provided the Earth-Ice model predictions for the study sites. This is a contribution to PALSEA and IGCP Project 588 "*Preparing for Coastal Change*". The manuscript benefited from the thoughtful and productive comments from Tom Cronin (USGS) two anonymous reviewers.

Table 1: Radiocarbon dates from cores LP-10 and CMC-8

Core – Depth (cm)	Sample ID	Radiocarbon Age (^{14}C years)	Radiocarbon Error (^{14}C years)	$\delta^{13}C$ (‰, VPDB)	Dated Material
LP10 – 127cm*	OS-70446	319	13	-12.41	Sp
LP10 – 135cm	OS-79171	415	25	-12.48	Ds
LP10 – 146cm	OS-79172	625	25	-12.77	Sp
LP10 – 184cm	OS-66518	950	30	-13.78	Sp
LP10 – 188cm	OS-79174	1090	25	-13.42	Sp
LP10 – 198cm	OS-70444	1188	30	-13.13	Sp
LP10 – 218cm*	OS-70442	1249	13	-13.89	Sp
LP10 – 226cm	OS-79175	1290	25	-13.88	Ds
LP10 – 237cm	OS-79176	1320	25	-13.86	Sp
LP10 – 245cm*‡	OS-70443	1502	14	-13.24	Sp
LP10 – 268cm*‡	OS-70445	1541	14	-14.57	Sp
LP10 – 282cm‡	OS-66514	1550	25	-14.4	Sp
LP10 – 295cm	OS-94847	1700	30	-23.99	Sa
LP10 – 300cm	OS-94846	1720	25	-26.82	Seed
LP10 – 307cm	OS-79177	1810	30	-24.66	Sa
LP10 – 314cm‡	OS-79178	1750	30	-26.47	Sa
LP10 – 327cm‡	OS-87528	1880	30	-12.69	HW
LP10 – 355cm	OS-94848	2190	25	-24.95	Pa
LP10 – 365cm	OS-87446	2230	25	-25.02	Sa
LP10 – 386cm	OS-94849	2210	35	-26.26	Pa
LP10 – 393cm	OS-87524	2450	25	-27.23	HW
CMC8 – 76cm	OS-94468	120	30	-11.15	Ds
CMC8 – 82cm	OS-94470	230	25	-10.97	Ds
CMC8 – 86cm	OS-88617	250	40	-10.07	Ds
CMC8 – 94cm	OS-94469	285	30	-10.47	Ds
CMC8 – 111cm	OS-88725	400	25	-24.92	Sp
CMC8 – 122cm	OS-88618	520	40	-13.82	Ds
CMC8 – 135cm	OS-79179	770	30	-13.45	Ds
CMC8 – 145cm	OS-79180	865	25	-13.61	Ds
CMC8 – 160cm	OS-88619	960	40	-13.94	Ds
CMC8 – 171cm	OS-79181	1100	30	-13.50	Ds
CMC8 – 180cm	OS-94471	1120	25	-12.60	Ds
CMC8 – 194cm	OS-88620	1190	35	-11.40	Sp
CMC8 – 208cm	OS-88726	1350	30	-27.73	Sa

All samples were dated by the National Oceanic Sciences Accelerator Mass Spectrometry facility, sample identifiers correspond to this lab. * denote dates that are not reported following standard rounding of radiocarbon age and error. Samples marked with ‡ were previously published in (Kemp et al., 2012c). Ds = *Distichlis spicata*; Spt = *Spartina patens*; HW = fragment of wood lying horizontal in core, Pa =

Phragmites australis; Sa = *Schoenoplectus americanus*. Reported $\delta^{13}C$ values are from an aliquot of CO_2 collected during sample combustion and refer only to the dated macrofossil and not the bulk sediment matrix from which it was isolated.

Table 2: Change Point Analysis

No. of Change Points	Converged?	Deviance Information Criterion (DIC)	Timing of Changes (AD)
0	Yes	-1843.9	
1	Yes	-1859.5	1922
2	Yes	-1886.3	897 and 1855
3	Yes	-1938.7	246, 733, and 1850
4	No	No convergence	
3 Change Point Model			
Interval	**Rate (mm/yr; 95% confidence)**	**Timing of Change (AD; 95% confidence)**	
i	-0.22 to -0.01		
ii	0.44 to 0.90	131-335	
iii	-0.18 to -0.07	633-825	
iv	2.81 to 3.47	1830-1873	

Results of change point analysis applied to the New Jersey sea-level reconstruction after 1.4mm/yr of estimated subsidence was removed. Models with 0, 1, 2, 3, and 4 change points were developed and checked for convergence, where the regression was forced to meet zero sea level in 2010AD. The Deviance Information Criterion (DIC) is a measure of model fit, where a lower value indicates a more robust fit to the data. The model with three change points was the best for describing sea-level changes in New Jersey. The 95% confidence interval for the four periods of persistent sea-level trends and timing of three change points is provided for the selected model.

Figure Captions

Figure 1: Location of study sites in New Jersey, USA (**A**). Distribution of modern foraminifera was documented at 12 sites (open circles (Kemp et al., 2013)), including five around Great Egg Harbor. Location of tide gauges at Cape May, NJ, Atlantic City, NJ, and Lewes, DE is denoted by T symbols. RMS = Rutgers Marine Station. Cores for sea-level reconstruction (filled circles) were collected at Leeds Point in the Edwin Forsythe National Wildlife Refuge (**B**) and at Cape May Courthouse (**C**).

Figure 2: Leeds Point Core 10 (LP-10). The abundance of the three most common species of foraminifera is represented by horizontal bars; *Miliammina petila* abundance is also shown. Stable carbon isotope concentrations ($\delta^{13}C$) for bulk sediment are parts per thousand (‰) relative to the Vienna Pee Dee Belemnite (VPDB) standard. Values corresponding to modern salt marsh (less depleted than -18.9‰) and highest salt marsh (more depleted than -22.0‰) environments dominated in New Jersey by C_4 and C_3 plants respectively are denoted by grey shading. Paleomarsh elevation (PME) was reconstructed using a transfer function applied to foraminifera preserved in core samples, SWLI = Standardized Water Level Index. Filled circles and error bars are sample-specific reconstructions of PME and uncertainty from the transfer function. Dashed lines display the error that was trimmed from the final reconstruction on the basis of $\delta^{13}C$ values. Minimum dissimilarity was measured using the Bray Curtis metric between each sample in the core and its single closest analogue in a training set of modern salt-marsh foraminifera from New Jersey. Vertical dashed lines mark thresholds for interpreting dissimilarity and were derived from pairwise analysis of the modern training set. The site of the closest analogue is shown by symbol shading. GB = Great Bay sites, EH = Egg Harbor Sites, BB = Brigantine Barrier, CMC = Cape May Courthouse. Goodness-of-fit to tidal elevation was measured as the squared residual fit of core samples in comparison to thresholds (vertical dashed lines) established from the modern dataset.

Figure 3: Cape May Courthouse Core 8 (CMC-8). The abundance of the three most common species of foraminifera is represented by grey horizontal bars. Stable carbon isotope concentrations ($\delta^{13}C$) for bulk sediment are parts per thousand (‰) relative to the Vienna Pee Dee Belemnite (VPDB) standard. Values corresponding to modern salt marsh (less depleted than -18.9‰) and highest salt marsh (more depleted than -22.0‰) environments dominated in New Jersey by C_4 and C_3 plants respectively are denoted by

grey shading. Paleomarsh elevation (PME) was reconstructed using a transfer function applied to foraminifera preserved in core samples, SWLI = Standardized Water Level Index. Filled circles and error bars are sample-specific reconstructions of PME and uncertainty from the transfer function. Dashed lines display the error that was trimmed from the final reconstruction on the basis of $\delta^{13}C$ values. Minimum dissimilarity was measured using the Bray Curtis metric between each sample in the core and its single closest analogue in a training set of modern salt-marsh foraminifera from New Jersey. Vertical dashed lines mark thresholds for interpreting dissimilarity and were derived from pairwise analysis of the modern training set. The site of the closest analogue is shown by symbol shading. GB = Great Bay sites, EH = Egg Harbor Sites, BB = Brigantine Barrier, CSG = Cold Spring. Goodness-of-fit to tidal elevation was measured as the squared residual fit of core samples in comparison to thresholds (vertical dashed lines) established from the modern dataset.

Figure 4: Chronology developed for core LP-10. Twenty one, identifiable plant macrofossils were radiocarbon dated and constrained the Bchron age model (shaded grey envelope). Solid horizontal bars represent the full range of calibrated ages rather than their probability distribution.

Figure 5: Chronohorizons in core CMC-8. **(A)** Downcore concentrations of elements (zinc, cadmium, copper, nickel and lead) and ratios of lead isotopes from bulk sediment (1cm thick) measured by mass spectrometry. Analytical errors are smaller than symbols. ^{137}Cs activity was calculated from gamma emission measurements. *Ambrosia* pollen is a marker for land clearance during European settlement. Grey bands with ages represent core intervals recognized as corresponding to prominent features in U.S. national production records **(B)**.

Figure 6: Chronology developed for core CMC-8. Thirteen, identifiable plant macrofossils were radiocarbon dated and constrained the Bchron age model (shaded grey envelope). Solid horizontal bars represent the full range of calibrated ages rather than their probability distribution. Pollution chronohorizons were recognized by downcore changes in elemental concentration, lead isotopic ratios and ^{137}Cs activity that could be related to features in historic production statistics. An increase in Ambrosia pollen was interpreted as being caused by land clearance during European settlement in the study region.

Figure 7: Relative sea-level reconstruction from southern New Jersey. **(A)** New index points from Leeds Point and Cape May Courthouse with vertical and age error reported following the same conventions as those from a database of radiocarbon dated index points in New Jersey. Relative sea-level predictions for Cape May Couthouse from the ICE6G-VM5b model are shown at 250 year time steps in as open circles **(B)** Relative sea level reconstructed from Leeds Point core 10 and Cape May Courthouse core 8 using foraminifera with stable carbon isotopes as sea level indicators and a composite chronology developed with Bchron age depth models to estimate sample age and uncertainty. Data points are represented by boxes that incorporate the vertical and temporal uncertainty from these two sources, but do not show associated probability distributions within each box.

Figure 8: (A) Tide-gauge records of relative sea level from sites in New Jersey and Delaware. Annual data computed from monthly means and plotted against the average for 2000-2010AD for each gauge. A single record was compiled by averaging annual data from the four gauges. A linear regression of the averaged record shows that relative sea level rose at average rate of 4.03mm/yr between 1911AD and 2012AD. **(B)** Comparison of the relative sea level reconstruction from Cape May Courthouse (dashed line) and a tide-gauge record produced by averaging annual data from Atlantic City, Sandy Hook, Cape May and Lewes (solid line). Tide-gauge data is relative to 2010AD (year of core collection). Age and vertical uncertainties from the sea-level reconstruction are represented by grey boxes.

Figure 9: New Jersey **(A)** and North Carolina **(B)** sea-level reconstructions with the estimated contribution of land-level change removed (1.4mm/yr for New Jersey and 0.9mm/yr or 1.0mm/yr for North Carolina). Data points previously represented by rectangles have been distorted into parallelograms by subtraction of a rate that has a larger effect on the older edge of each box than it does on the younger edge. Average rates of sea-level change for four persistent phases are listed and the 95% confidence interval for the timing of rate changes are represented by probability distributions. The shaded bands are the best-fit change point regressions. The same change point model was applied to both records, causing marginally different results for North Carolina than those originally reported by (Kemp et al., 2011).

References

Ahmed, M., Anchukaitis, K.J., Asrat, A., Borgaonkar, H.P., Braida, M., Buckley, B.M., Buntgen, U., Chase, B.M., Christie, D.A., Cook, E.R., Curran, M.A.J., Diaz, H.F., Esper, J., Fan, Z.-X., Gaire, N.P., Ge, Q., Gergis, J., Gonzalez-Rouco, J.F., Goosse, H., Grab, S.W., Graham, N., Graham, R., Grosjean, M., Hanhijarvi, S.T., Kaufman, D.S., Kiefer, T., Kimura, K., Korhola, A.A., Krusic, P.J., Lara, A., Lezine, A.-M., Ljungqvist, F.C., Lorrey, A.M., Luterbacher, J., Masson-Delmotte, V., McCarroll, D., McConnell, J.R., McKay, N.P., Morales, M.S., Moy, A.D., Mulvaney, R., Mundo, I.A., Nakatsuka, T., Nash, D.J., Neukom, R., Nicholson, S.E., Oerter, H., Palmer, J.G., Phipps, S.J., Prieto, M.R., Rivera, A., Sano, M., Severi, M., Shanahan, T.M., Shao, X., Shi, F., Sigl, M., Smerdon, J.E., Solomina, O.N., Steig, E.J., Stenni, B., Thamban, M., Trouet, V., Turney, C.S.M., Umer, M., van Ommen, T., Verschuren, D., Viau, A.E., Villalba, R., Vinther, B.M., von Gunten, L., Wagner, S., Wahl, E.R., Wanner, H., Werner, J.P., White, J.W.C., Yasue, K., Zorita, E., 2013. Continental-scale temperature variability during the past two millennia. Nature Geoscience advance online publication.

Ault, W.U., Senechal, R.G., Erlebach, W.E., 1970. Isotopic composition as a natural tracer of lead in the environment. Environmental Science & Technology 4, 305-313.

Barlow, N.L.M., Shennan, I., Long, A.J., Gehrels, W.R., Saher, M.H., Woodroffe, S.A., Hillier, C., 2013. Salt marshes as late Holocene tide gauges. Global and Planetary Change 106, 90-110.

Benner, R., Fogel, M.L., Sprague, E.K., 1991. Diagenesis of belowground biomass of *Spartina alterniflora* in salt-marsh sediments. Limnology and Oceanography 36, 1358-1374.

Benner, R., Fogel, M.L., Sprague, E.K., Hodson, R.E., 1987. Depletion of ^{13}C in lignin and its implications for stable isotope studies. Nature 329, 708-710.

Bindoff, N.L., Willebrand, J., Artale, V., A, C., Gregory, J., Gulev, S., Hanawa, K., Quéré, C.L., Levitus, S., Nojiri, Y., Shum, C.K., L.D.Talley, Unnikrishnan, A., 2007. Observations: Oceanic Climate Change and Sea Level, In: Solomon, S., Qin, D., Mannin, M., Chen, Z., Marquis, M., Avery, K.B., Tignor, M., Miller, H.L. (Eds.), Climate Change 2007: The Physical Science Basis. Contribution of Working Group I to the Fourth Assessment Report of the Intergovernmental Panel on Climate Change Cambridge University Press, Cambridge.

Bingham, R.J., Hughes, C.W., 2009. Signature of the Atlantic meridional overturning circulation in sea level along the east coast of North America. Geophysical Research Letters 36, L02603.

Birks, H.J.B., 1998. Numerical tools in paleolimnology - progress, potentialities and problems. Journal of Paleolimnology 20, 307-332.

Bittermann, K., Rahmstorf, S., Perrette, M., Vermeer, M., 2013. Predictability of twentieth century sea-level rise from past data. Environmental Research Letters 8, 014013.

Bleiwas, D.I., DiFrancesco, C., 2010. Historical zinc smelting in New Jersey, Pennsylvania, Virginia, West Virginia, and Washington, D.C., with estimates of atmospheric zinc emissions and other materials, Open File Report 2010-1131. United States Geological Survey, p. 189.

Bollhöfer, A., Rosman, K.J.R., 2001. Isotopic source signatures for atmospheric lead: the Northern Hemisphere. Geochimica et Cosmochimica Acta 65, 1727-1740.

Boon, J.D., 2012. Evidence of sea level acceleration at U.S. and Canadian tide stations, Atlantic coast, North America. Journal of Coastal Research 28, 1437-1445.

Brain, M.J., Long, A.J., Woodroffe, S.A., Petley, D.N., Milledge, D.G., Parnell, A.C., 2012. Modelling the effects of sediment compaction on salt marsh reconstructions of recent sea-level rise. Earth and Planetary Science Letters 345-348, 180-193.

Byrne, R., Ingram, B.L., Starratt, S., Malamud-Roam, F., Collins, J.N., Conrad, M.E., 2001. Carbon-Isotope, Diatom, and Pollen Evidence for Late Holocene Salinity Change in a Brackish Marsh in the San Francisco Estuary. Quaternary Research 55, 66-76.

Cazenave, A., Llovel, W., 2010. Contemporary sea level rise. Annual Review of Marine Science 2, 145-173.

Chmura, G.L., Aharon, P., 1995. Stable carbon isotope signatures of sedimentary carbon in coastal wetlands as indicators of salinity regime. Journal of Coastal Research 11, 124-135.

Church, J., White, N., Aarup, T., Wilson, W., Woodworth, P., Domingues, C., Hunter, J., Lambeck, K., 2008. Understanding global sea levels: past, present and future. Sustainability Science 3, 9-22.

Church, J.A., White, N.J., 2006. A 20th century acceleration in global sea-level rise. Geophysical Research Letters 33, L01602.

Church, J.A., White, N.J., 2011. Sea-level rise from the late 19th to the early 21st century. Surveys in Geophysics 32, 585-602.

Cronin, T.M., 2012. Rapid sea-level rise. Quaternary Science Reviews 56, 11-30.

Daddario, J.J., 1961. A lagoon deposit profile near Atlantic City, New Jersey. Bulletin of the New Jersey Academy of Science 6, 7-14.

Davis, G.H., 1987. Land subsidence and sea level rise on the Atlantic Coastal Plain of the United States. Environmental Geology and Water Sciences 10, 67-80.

Donnelly, J.P., Cleary, P., Newby, P., Ettinger, R., 2004. Coupling instrumental and geological records of sea-level change: evidence from southern New England of an increase in the rate of sea-level rise in the late 19th century. Geophysical Research Letters 31, L05203.

Ember, L.M., Williams, D.F., Morris, J.T., 1987. Processes that influence carbon isotope variations in salt marsh sediments. Marine Ecology Progress Series 36, 33-42.

Engelhart, S.E., Horton, B.P., 2012. Holocene sea level database for the Atlantic coast of the United States. Quaternary Science Reviews 54, 12-25.

Engelhart, S.E., Horton, B.P., Douglas, B.C., Peltier, W.R., Tornqvist, T.E., 2009. Spatial variability of late Holocene and 20th century sea-level rise along the Atlantic coast of the United States. Geology 37, 1115-1118.

Engelhart, S.E., Horton, B.P., Kemp, A.C., 2011a. Holocene sea level changes along the United States' Atlantic Coast. Oceanography 24, 70-79.

Engelhart, S.E., Peltier, W.R., Horton, B.P., 2011b. Holocene relative sea-level changes and glacial isostatic adjustment of the U.S. Atlantic coast. Geology 39, 751-754.

Ezer, T., Atkinson, L.P., Corlett, W.B., Blanco, J.L., 2013. Gulf Stream's induced sea level rise and variability along the U.S. mid-Atlantic coast. Journal of Geophysical Research: Oceans 118, 685-697.

Ferland, M.A., 1990. Holocene depositional history of the southern New Jersey barrier and back barrier regions. US Army Corps of Engineers, p. 75.

Fogel, M.L., Kent Sprague, E., Gize, A.P., Frey, R.W., 1989. Diagenesis of organic matter in Georgia salt marshes. Estuarine, Coastal and Shelf Science 28, 211-230.

Gehrels, W.R., 2000. Using foraminiferal transfer functions to produce high-resolution sea-level records from salt-marsh deposits, Maine, USA. The Holocene 10, 367-376.

Gehrels, W.R., Callard, S.L., Moss, P.T., Marshall, W.A., Blaauw, M., Hunter, J., Milton, J.A., Garnett, M.H., 2012. Nineteenth and twentieth century sea-level changes in Tasmania and New Zealand. Earth and Planetary Science Letters 315-316, 94-102.

Gehrels, W.R., Hayward, B., Newnham, R.M., Southall, K.E., 2008. A 20th century acceleration of sea-level rise in New Zealand. Geophysical Research Letters 35, L02717.

Gehrels, W.R., Kirby, J.R., Prokoph, A., Newnham, R.M., Achterberg, E.P., Evans, H., Black, S., Scott, D.B., 2005. Onset of recent rapid sea-level rise in the western Atlantic Ocean. Quaternary Science Reviews 24, 2083-2100.

Gehrels, W.R., Woodworth, P.L., 2012. When did modern rates of sea-level rise start? Global and Planetary Change 100, 263-277.

Gobeil, C., Tessier, A., Couture, R.-M., 2013. Upper Mississippi Pb as a mid-1800s chronostratigraphic marker in sediments from seasonally anoxic lakes in Eastern Canada. Geochimica et Cosmochimica Acta 113, 125-135.
Goñi, M., Thomas, K., 2000. Sources and transformations of organic matter in surface soils and sediments from a tidal estuary (North Inlet, South Carolina, USA). Estuaries and Coasts 23, 548-564.
González, J.L., Törnqvist, T.E., 2009. A new Late Holocene sea-level record from the Mississippi Delta: evidence for a climate/sea level connection? Quaternary Science Reviews 28, 1737-1749.
Graney, J.R., Halliday, A.N., Keeler, G.J., Nriagu, J.O., Robbins, J.A., Norton, S.A., 1995. Isotopic record of lead pollution in lake sediments from the northeastern United States. Geochimica et Cosmochimica Acta 59, 1715-1728.
Haslett, J., Parnell, A., 2008. A simple monotone process with application to radiocarbon-dated depth chronologies. Journal of the Royal Statistical Society: Series C (Applied Statistics) 57, 399-418.
Horton, B., Engelhart, S.E., Hill, D.F., Kemp, A.C., Nikitina, D.L., Miller, K.G., Peltier, R.W., 2013. Influence of tidal-range change and sediment compaction on Holocene relative sea-level change in New Jersey, USA. Journal of Quaternary Science 28, 403-411.
Horton, B.P., Edwards, R.J., 2006. Quantifying Holocene sea-level change using intertidal foraminifera: lessons from the British Isles. Cushman Foundation for Foraminiferal Research, Special Publication 40, 97.
Jevrejeva, S., Moore, J.C., Grinsted, A., Woodworth, P.L., 2008. Recent global sea level acceleration started over 200 years ago? Geophysical Research Letters 35, L08715.
Johnson, B.J., Moore, K.A., Lehmann, C., Bohlen, C., Brown, T.A., 2007. Middle to late Holocene fluctuations of C_3 and C_4 vegetation in a Northern New England Salt Marsh, Sprague Marsh, Phippsburg Maine. Organic Geochemistry 38, 394-403.
Kemp, A.C., Horton, B., Donnelly, J.P., Mann, M.E., Vermeer, M., Rahmstorf, S., 2011. Climate related sea-level variations over the past two millennia. Proceedings of the National Academy of Sciences 108, 11017-11022.
Kemp, A.C., Horton, B.P., Vann, D.R., Engelhart, S.E., Vane, C.H., Nikitina, D., Anisfeld, S.C., 2012a. Quantitative vertical zonation of salt-marsh foraminifera for reconstructing former sea level; an example from New Jersey, USA. Quaternary Science Reviews 54, 26-39.
Kemp, A.C., Sommerfield, C.K., Vane, C.H., Horton, B.P., Chenery, S.R., Anisfeld, S.C., Nikitina, D., 2012b. Use of lead isotopes for developing chronologies in recent salt-marsh sediments. Quaternary Geochronology 12, 40-49.
Kemp, A.C., Telford, R.J., Horton, B.P., Anisfeld, S.C., Sommerfield, C.K., 2013. Reconstructing Holocene sea-level using salt-marsh foraminifera and transfer functions: lessons from New Jersey, USA. Journal of Quaternary Science 28, 617-629.
Kemp, A.C., Vane, C.H., Horton, B.P., Engelhart, S.E., Nikitina, D., 2012c. Application of stable carbon isotopes for reconstructing salt-marsh floral zones and relative sea level, New Jersey, USA. Journal of Quaternary Science 27, 404-414.
Kienert, H., Rahmstorf, S., 2012. On the relation between Meridional Overturning Circulation and sea-level gradients in the Atlantic. Earth System Dynamics 3, 109-120.
Lamb, A.L., Wilson, G.P., Leng, M.J., 2006. A review of coastal palaeoclimate and relative sea-level reconstructions using $\delta^{13}C$ and C/N ratios in organic material. Earth-Science Reviews 75, 29-57.
Lima, A.L., Bergquist, B.A., Boyle, E.A., Reuer, M.K., Dudas, F.O., Reddy, C.M., Eglinton, T.I., 2005. High-resolution historical records from Pettaquamscutt River basin sediments: 2. Pb isotopes reveal a potential new stratigraphic marker. Geochimica et Cosmochimica Acta 69, 1813-1824.
Malamud-Roam, F., Ingram, B.L., 2004. Late Holocene $\delta^{13}C$ and pollen records of paleosalinity from tidal marshes in the San Francisco Bay estuary, California. Quaternary Research 62, 134-145.

Mann, M.E., Zhang, Z., Hughes, M.K., Bradley, R.S., Miller, S.K., Rutherford, S., Ni, F., 2008. Proxy-based reconstructions of hemispheric and global surface temperature variations over the past two millennia. Proceedings of the National Academy of Sciences 105, 13252-13257.

Marshall, W.A., Gehrels, W.R., Garnett, M.H., Freeman, S.P.H.T., Maden, C., Xu, S., 2007. The use of 'bomb spike' calibration and high-precision AMS C-14 analyses to date salt-marsh sediments deposited during the past three centuries. Quaternary Research 68, 325-337.

Meyerson, A.L., 1972. Pollen and paleosalinity analyses from a Holocene tidal marsh sequence, Cape May County, New Jersey. Marine Geology 12, 335-357.

Middleburg, J.J., Nieuwenhuize, J., Lubberts, R.K., van de Plassche, O., 1997. Organic carbon isotope systematics of coastal marshes. Estuarine Coastal and Shelf Science 45, 681-687.

Miller, K.G., Sugarman, P.J., Browning, J.V., Horton, B.P., Stanley, A., Kahn, A., Uptegrove, J., Aucott, M., 2009. Sea-level rise in New Jersey over the past 5000 years: Implications to anthropogenic changes. Global and Planetary Change 66, 10-18.

Moberg, A., Sonechkin, D.M., Holmgren, K., Datsenko, N.M., Karlen, W., 2005. Highly variable Northern Hemisphere temperatures reconstructed from low- and high-resolution proxy data. Nature 433, 613-617.

Morris, J.T., Sundareshwar, P.V., Nietch, C.T., Kjerfve, B., Cahoon, D.R., 2002. Response of coastal wetlands to rising sea level. Ecology 83, 2869-2877.

Parnell, A.C., Haslett, J., Allen, J.R.M., Buck, C.E., Huntley, B., 2008. A flexible approach to assessing synchroneity of past events using Bayesian reconstructions of sedimentation history. Quaternary Science Reviews 27, 1872-1885.

Psuty, N.P., 1986. Holocene sea level in New Jersey. Physical Geography 7, 156-167.

Rahmstorf, S., 2007. A semi-empirical approach to projecting future sea-level rise. Science 315, 368-370.

Reimer, P.J., Baillie, M.G.L., Bard, E., Bayliss, A., Beck, J.W., Blackwell, P.G., Ramsey, C.B., Buck, C.E., Burr, G.S., Edwards, R.L., Friedrich, M., Grootes, P.M., Guilderson, T.P., Hajdas, I., Heaton, T.J., Hogg, A.G., Hughen, K.A., Kaiser, K.F., Kromer, B., McCormac, F.G., Manning, S.W., Reimer, R.W., Richards, D.A., Southon, J.R., Talamo, S., Turney, C.S.M., van der Plicht, J., Weyhenmeyer, C.E., 2011. IntCal09 and Marine09 radiocarbon age calibration curves, 0-50,000 years cal. BP. Radiocarbon 51, 1111-1150.

Sallenger, A.H., Doran, K.S., Howd, P.A., 2012. Hotspot of accelerated sea-level rise on the Atlantic coast of North America. Nature Climate Change 2, 884-888.

Scott, D.B., Medioli, F.S., 1978. Vertical zonations of marsh foraminifera as accurate indicators of former sea levels. Nature 272, 528-531.

Shennan, I., Milne, G., Bradley, S., 2012. Late Holocene vertical land motion and relative sea-level changes: lessons from the British Isles. Journal of Quaternary Science 27, 64-70.

Simpson, G.L., 2007. Analogue Methods in Palaeoecology: Using the analogue Package. Journal of Statistical Software 22, 1-29.

Simpson, G.L., Hall, R.I., 2012. Human impacts: applications of numerical methods to evaluate surface water acidification and eutrophication, In: Birks, H.J.B., Lotter, A.F., Juggins, S., Smol, J.P. (Eds.), Data handling and numerical techniques. Springer, pp. 579-614.

Sivan, D., Lambeck, K., Toueg, R., Raban, A., Porath, Y., Shirman, B., 2004. Ancient coastal wells of Caesarea Maritima, Israel, an indicator for relative sea level changes during the last 2000 years. Earth and Planetary Science Letters 222, 315-330.

Spiegelhalter, D.J., Best, N.G., Carlin, B.P., Van Der Linde, A., 2002. Bayesian measures of model complexity and fit. Journal of the Royal Statistical Society: Series B (Statistical Methodology) 64, 583-639.

Stuckey, I.H., Gould, L.L., 2000. Coastal plants from Cape Cod to Cape Canaveral. University of North Carolina Press, Chapel Hill.

Sun, H., Grandstaff, D., Shagam, R., 1999. Land subsidence due to groundwater withdrawal: potential damage of subsidence and sea level rise in southern New Jersey, USA. Environmental Geology 37, 290-296.

Tanner, B.R., Uhle, M.E., Mora, C.I., Kelley, J.T., Schuneman, P.J., Lane, C.S., Allen, E.S., 2010. Comparison of bulk and compound-specific $\delta^{13}C$ analyses and determination of carbon sources to salt marsh sediments using n-alkane distributions (Maine, USA). Estuarine, Coastal and Shelf Science 86, 283-291.

Thomas, E., Varekamp, J., 1991. Paleo-environmental analysis of marsh sequences (Clinton, CT); evidence for punctuated sea-level rise during the latest Holocene. Journal of Coastal Research 11, 125-158.

Thompson, L.G., Mosley-Thompson, E., Davis, M.E., Zagorodnov, V.S., Howat, I.M., Mikhalenko, V.N., Lin, P.N., 2013. Annually resolved ice core records of tropical climate variability over the past ~1800 years. Science.

Tiner, R.W., 1985. Wetlands of New Jersey, In: Service, U.S.F.a.W. (Ed.), National Wetlands Inventory. U.S. Fish and Wildlife Service, Newton Corner, MA, p. 117.

Traverse, A., 2007. Paleopalynology. Springer.

van de Plassche, O., 2000. North Atlantic Climate-Ocean Variations and Sea Level in Long Island Sound, Connecticut, Since 500 cal yr A.D. Quaternary Research 53, 89-97.

van de Plassche, O., Erkens, G., van Vliet, F., Brandsma, J., van der Borg, K., de Jong, A.F.M., 2006. Salt-marsh erosion associated with hurricane landfall in southern New England in the fifteenth and seventeenth centuries. Geology 34, 829-832.

van de Plassche, O., van der Borg, K., de Jong, A.F.M., 1998. Sea level-climate correlation during the past 1400 yr. Geology 26, 319-322.

Vane, C.H., Chenery, S.R., Harrison, I., Kim, A.W., Moss-Hayes, V., Jones, D.G., 2011. Chemical signatures of the Anthropocene in the Clyde estuary, UK: sediment-hosted Pb, 207/206Pb, total petroleum hydrocarbon, polyaromatic hydrocarbon and polychlorinated biphenyl pollution records. Philosophical Transactions of the Royal Society A: Mathematical, Physical and Engineering Sciences 369, 1085-1111.

Vane, C.H., Jones, D.G., Lister, T.R., 2009. Mercury contamination in surface sediments and sediment cores of the Mersey Estuary, UK. Marine Pollution Bulletin 58, 940-946.

Vane, C.H., Kim, A.W., Moss-Hayes, V., Snape, C.E., Diaz, M.C., Khan, N.S., Engelhart, S.E., Horton, B.P., 2013. Degradation of mangrove tissues by arboreal termites (Nasutitermes acajutlae) and their role in the mangrove C cycle (Puerto Rico): Chemical characterization and organic matter provenance using bulk δ13C, C/N, alkaline CuO oxidation-GC/MS, and solid-state 13C NMR. Geochemistry, Geophysics, Geosystems, n/a-n/a.

Wacker, P.O., 1975. Land and people: a cultural geography of preindustrial New Jersey: origins and settlement patterns. Rutgers University Press, Newark, NJ.

Wacker, P.O., Clemens, P.G.E., 1994. Land use in early New Jersey; a historical geography. Rutgers University Press, Newark, NJ.

Warneke, T., Croudace, I.W., Warwick, P.E., Taylor, R.N., 2002. A new ground-level fallout record of uranium and plutonium isotopes for northern temperate latitudes. Earth and Planetary Science Letters 203, 1047-1057.

Wilson, G.P., Lamb, A.L., Leng, M.J., Gonzalez, S., Huddart, D., 2005. $\delta^{13}C$ and C/N as potential coastal palaeoenvironmental indicators in the Mersey Estuary, UK. Quaternary Science Reviews 24, 2015-2029.

Yang, Z., Myers, E.P., Wong, A., White, S., 2008. Vdatum for Chesapeake Bay, Delaware Bay, and Adjacent Coastal Water Areas: Tidal Datums and Sea surface Topography, NOAA Technical Memorandum NOS CS 15. U.S. Department of Commerce, National Oceanic and Atmospheric Administration, Silver Spring, Maryland, p. 110.

Yin, J., Schlesinger, M.E., Stouffer, R.J., 2009. Model projections of rapid sea-level rise on the northeast coast of the United States. Nature Geoscience 2, 262-266.

1016

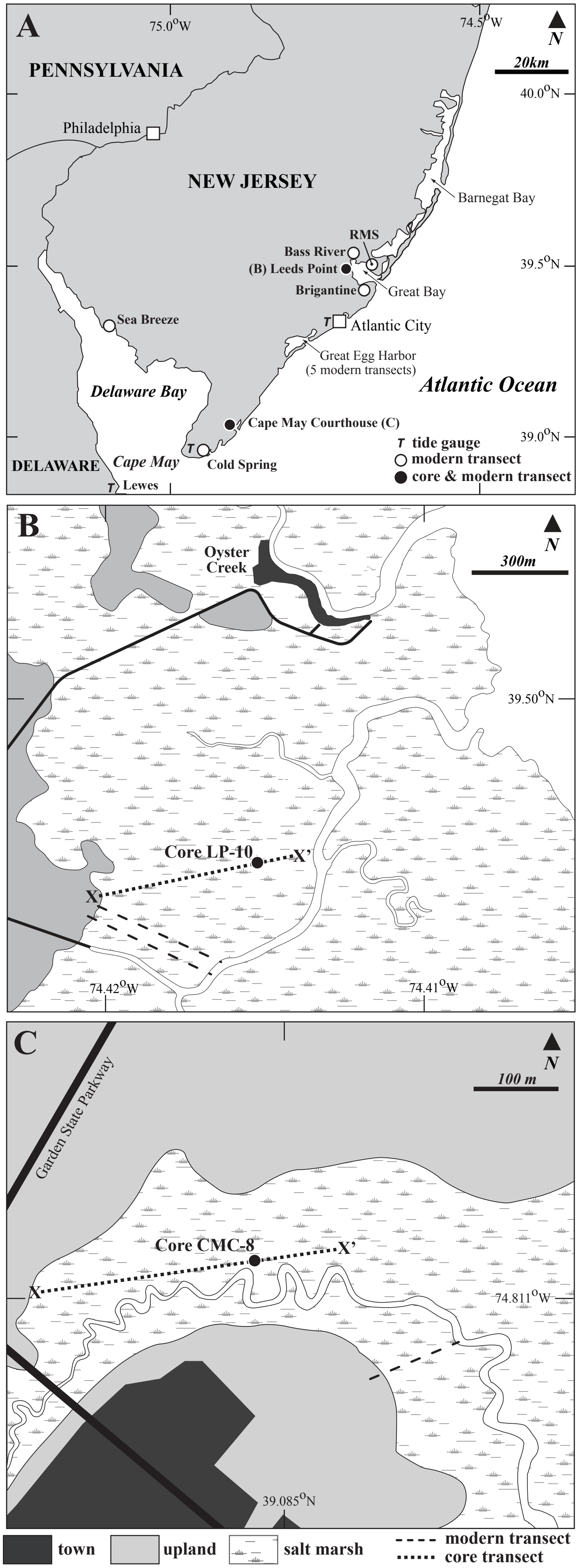

A
75.0°W
74.5°W
N
20km
PENNSYLVANIA
40.0°N
Philadelphia
NEW JERSEY
Barnegat Bay
RMS
Bass River
(B) Leeds Point
39.5°N
Brigantine
Great Bay
T
Atlantic City
Sea Breeze
Great Egg Harbor
(5 modern transects)
Delaware Bay
Atlantic Ocean
Cape May Courthouse (C)
39.0°N
T tide gauge
modern transect
core & modern transect
DELAWARE
Cape May
Cold Spring
Lewes
B
N
300m
Oyster
Creek
39.50°N
Core LP-10
X'
X
74.42°W
74.41°W
C
N
100 m
Garden State Parkway
Core CMC-8
X'
X
74.811°W
39.085°N
town
upland
salt marsh
modern transect
core transect

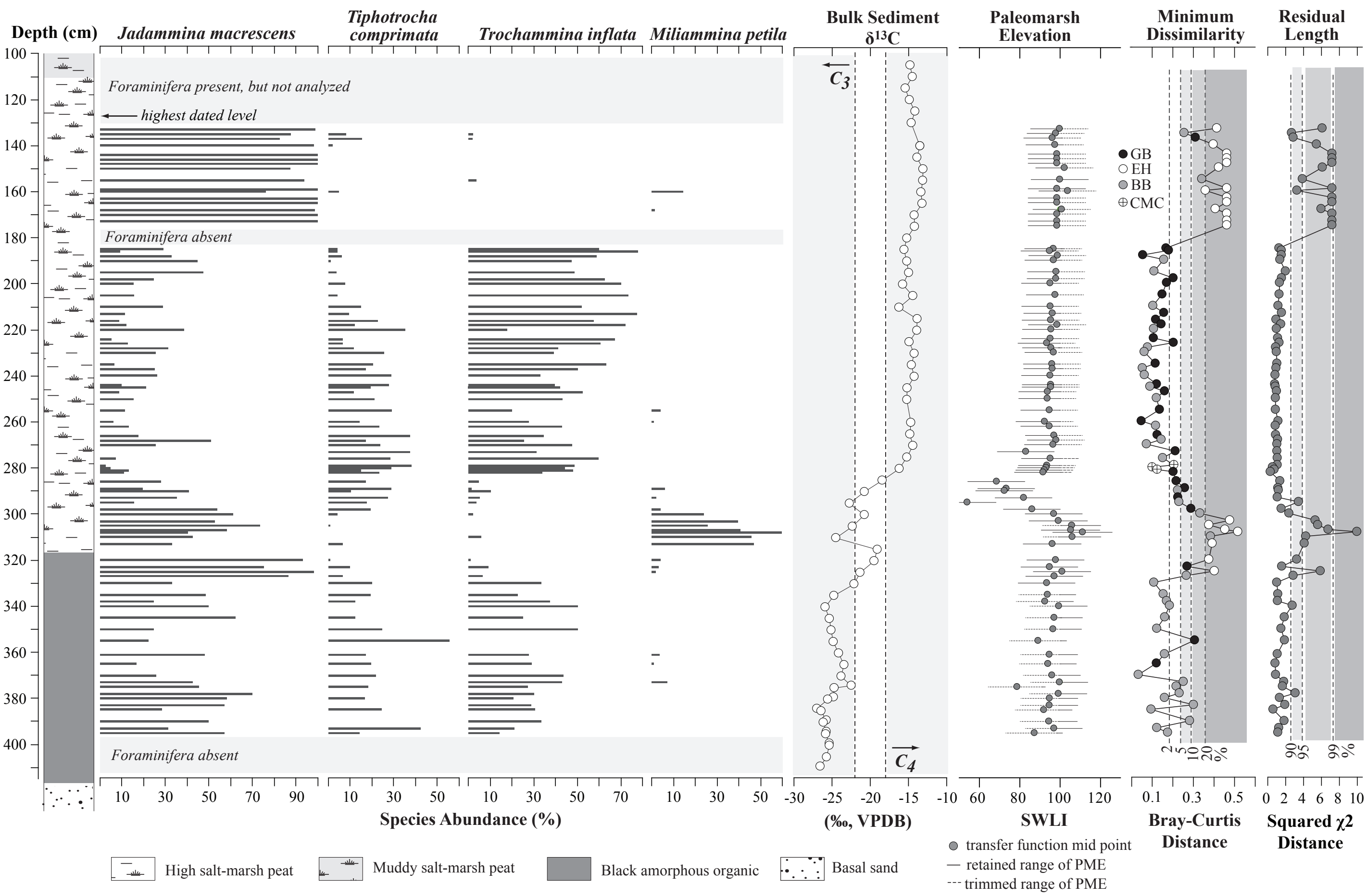

Depth (cm)
Jadammina macrescens
Tiphotrocha comprimata
Trochammina inflata
Miliammina petila
Bulk Sediment δ13C
Paleomarsh Elevation
Minimum Dissimilarity
Residual Length
Foraminifera present, but not analyzed
highest dated level
Foraminifera absent
Foraminifera absent
C3
C4
GB
EH
BB
CMC
Species Abundance (%)
(‰, VPDB)
SWLI
Bray-Curtis Distance
Squared χ2 Distance
High salt-marsh peat
Muddy salt-marsh peat
Black amorphous organic
Basal sand
transfer function mid point
retained range of PME
trimmed range of PME

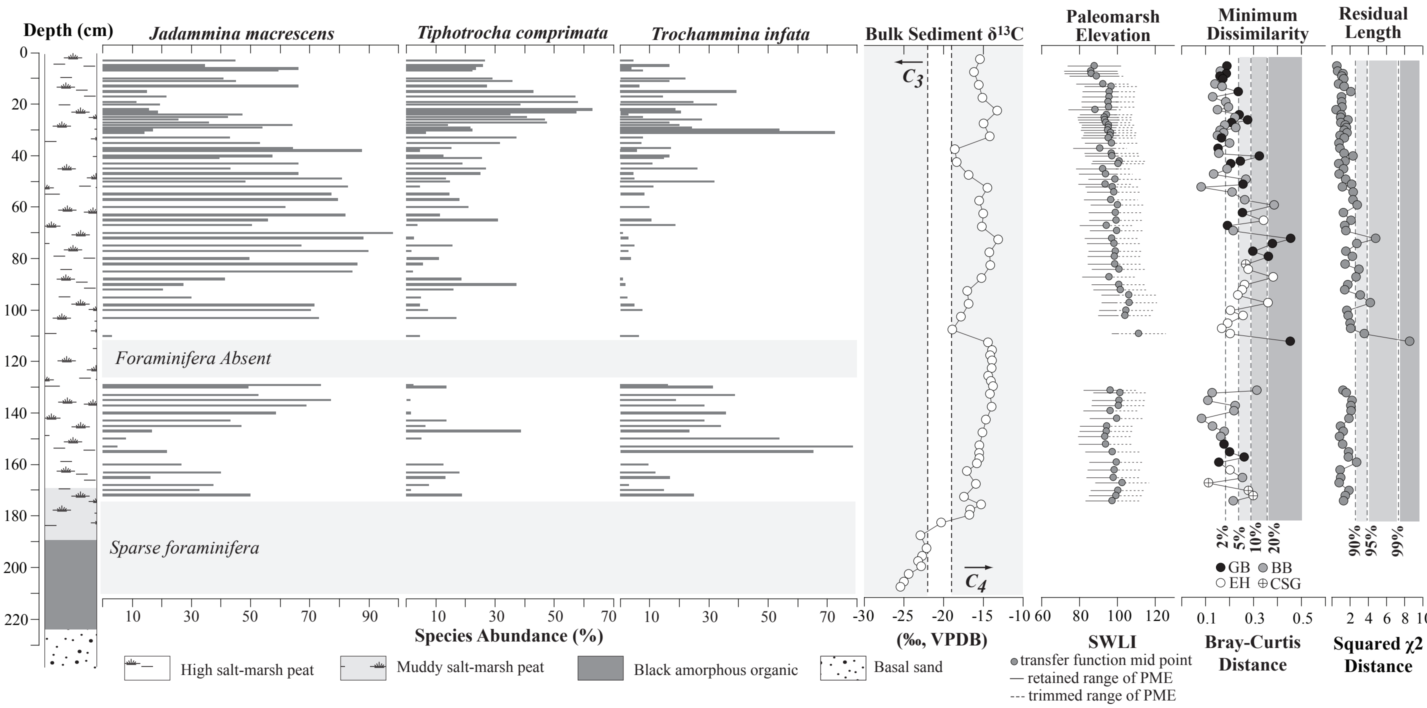
Depth (cm)
Jadammina macrescens
Tiphotrocha comprimata
Trochammina infata
Bulk Sediment δ13C
C3
C4
Paleomarsh Elevation
Minimum Dissimilarity
Residual Length
Foraminifera Absent
Sparse foraminifera
Species Abundance (%)
(‰, VPDB)
SWLI
Bray-Curtis Distance
Squared χ2 Distance
2%
5%
10%
20%
90%
95%
99%
GB
BB
EH
CSG
High salt-marsh peat
Muddy salt-marsh peat
Black amorphous organic
Basal sand
transfer function mid point
— retained range of PME
--- trimmed range of PME

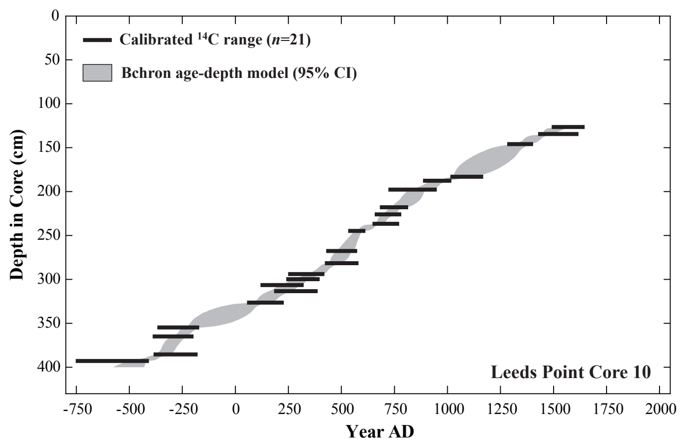
Calibrated ^{14}C range (n=21)
Bchron age-depth model (95% CI)
Leeds Point Core 10
Depth in Core (cm)
Year AD
0
50
100
150
200
250
300
350
400
-750
-500
-250
0
250
500
750
1000
1250
1500
1750
2000

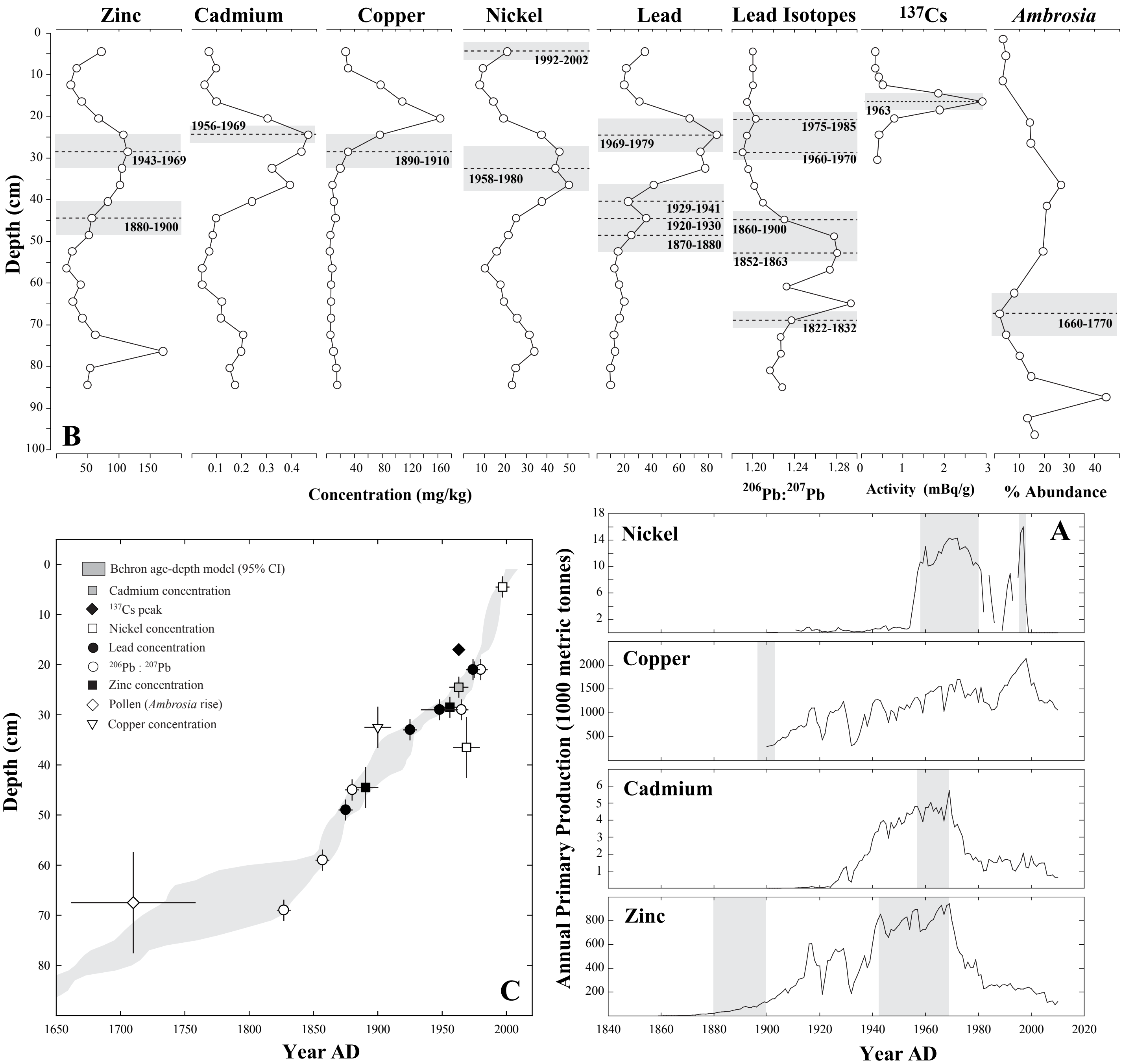

Zinc
Cadmium
Copper
Nickel
Lead
Lead Isotopes
137Cs
Ambrosia
Depth (cm)
1943-1969
1880-1900
1956-1969
1890-1910
1992-2002
1958-1980
1969-1979
1929-1941
1920-1930
1870-1880
1975-1985
1960-1970
1860-1900
1852-1863
1822-1832
1963
1660-1770
B
Concentration (mg/kg)
206Pb:207Pb
Activity (mBq/g)
% Abundance
Bchron age-depth model (95% CI)
Cadmium concentration
137Cs peak
Nickel concentration
Lead concentration
206Pb : 207Pb
Zinc concentration
Pollen (Ambrosia rise)
Copper concentration
C
Year AD
Nickel
A
Copper
Cadmium
Zinc
Annual Primary Production (1000 metric tonnes)
Year AD

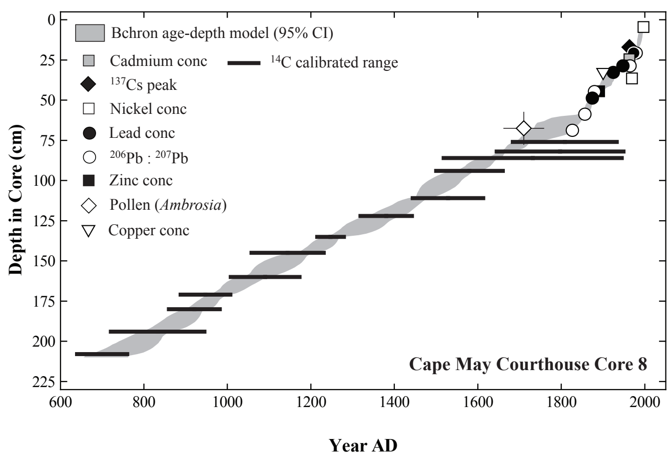

Bchron age-depth model (95% CI)
Cadmium conc
^{14}C calibrated range
^{137}Cs peak
Nickel conc
Lead conc
^{206}Pb : ^{207}Pb
Zinc conc
Pollen (*Ambrosia*)
Copper conc
Cape May Courthouse Core 8
Depth in Core (cm)
Year AD
0
25
50
75
100
125
150
175
200
225
600
800
1000
1200
1400
1600
1800
2000

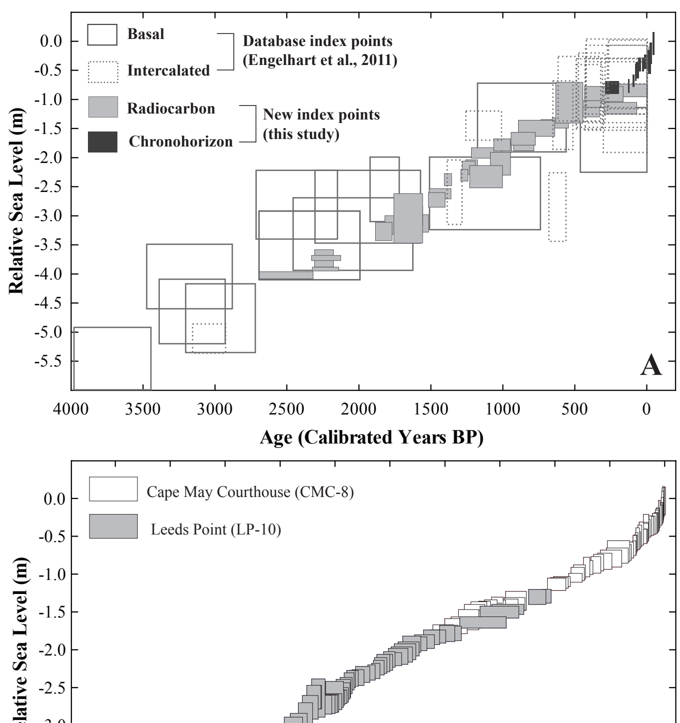

Basal
Intercalated
Database index points
(Engelhart et al., 2011)
Radiocarbon
Chronohorizon
New index points
(this study)
Relative Sea Level (m)
A
Age (Calibrated Years BP)
Cape May Courthouse (CMC-8)
Leeds Point (LP-10)
Relative Sea Level (m)
B
Year (AD)

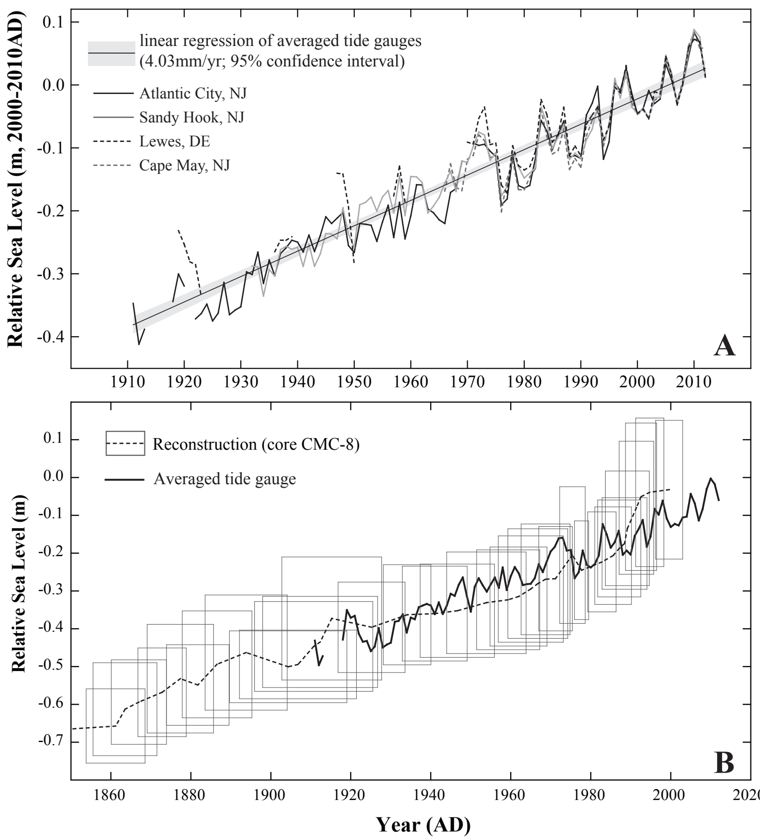
linear regression of averaged tide gauges
(4.03mm/yr; 95% confidence interval)
Atlantic City, NJ
Sandy Hook, NJ
Lewes, DE
Cape May, NJ
Relative Sea Level (m, 2000-2010AD)
A
Reconstruction (core CMC-8)
Averaged tide gauge
Relative Sea Level (m)
B
Year (AD)

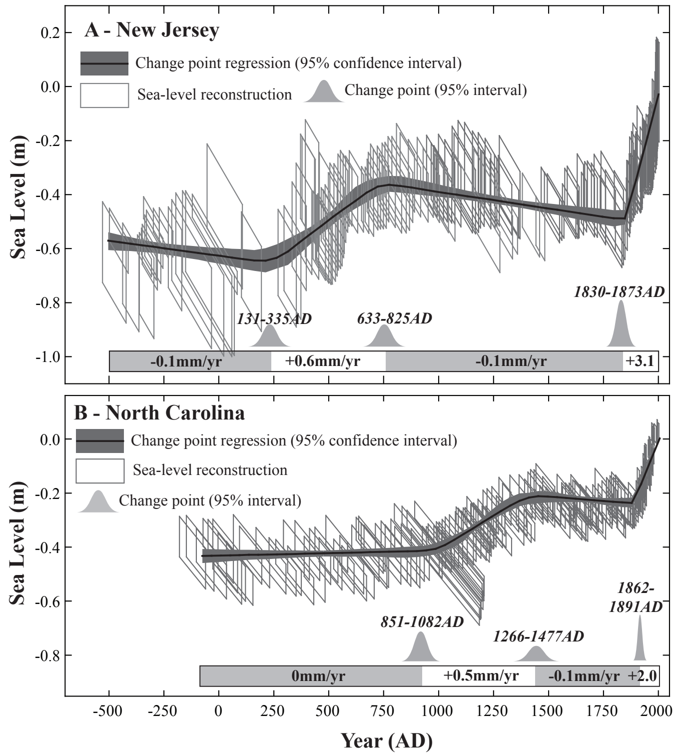
A - New Jersey
Change point regression (95% confidence interval)
Sea-level reconstruction
Change point (95% interval)
Sea Level (m)
0.2
0.0
-0.2
-0.4
-0.6
-0.8
-1.0
1830-1873AD
131-335AD
633-825AD
-0.1mm/yr
+0.6mm/yr
-0.1mm/yr
+3.1
B - North Carolina
Change point regression (95% confidence interval)
Sea-level reconstruction
Change point (95% interval)
Sea Level (m)
0.0
-0.2
-0.4
-0.6
-0.8
1862-
1891AD
851-1082AD
1266-1477AD
0mm/yr
+0.5mm/yr
-0.1mm/yr
+2.0
-500
-250
0
250
500
750
1000
1250
1500
1750
2000
Year (AD)